INTERNATIONAL ATOMIC ENERGY AGENCY
UNITED NATIONS EDUCATIONAL, SCIENTIFIC AND CULTURAL ORGANIZATION
INTERNATIONAL CENTRE FOR THEORETICAL PHYSICS
I.C.T.P., P.O. BOX 586, 34100 TRIESTE, ITALY, CABLE: CENTRATOM TRIESTE

UNITED NATIONS INDUSTRIAL DEVELOPMENT ORGANIZATION

INTERNATIONAL CENTRE FOR SCIENCE AND HIGH TECHNOLOGY

H4.SMR/540-18

Second Training College on Physics and Technology of Lasers and Optical Fibres

21 January - 15 February 1991

Lasers for Optical Communications

H. Burkhard
German Telecom Research Institute
Darmstadt, D-6100
Germany

Lasers for Optical Communications

H. Burkhard, DBP TELEKOM Forschungsinstitut beim FTZ, P.O. Box 10 00 03
D-6100 Darmstadt, FRG

DFB/DBR laser

For optoelectronic integration Fabry Perot type lasers with etched or cleaved facets are not well suited. Dynamical single mode behaviour has to be achieved by a wavelength selective feedback. The DFB and DBR concepts are well suited.

DFB lasers

DFB lasers with gratings of the first Bragg order and antireflection coatings do not oscillate at the Bragg wavelength. There is a stop band depending on the strength of the coupling of the light to the grating. Below and above the stop band borders two modes oscillate simultaneously. Means for discrimination of one of the modes have to be found. Different methods have been proposed for the removal of the degeneracy of the threshold gain:

1) antisymmetric taper in the coupling coefficient,
2) chirped grating: Λ or n_{eff} varies slowly along the axis,
3) $\pi/2$ phase shift of the grating,
4) short area in the waveguide with changed stripewidth: $\pi/2$ phase shift,
5) different reflectivities at the endfacets.

DFB lasers with gratings of second order

The methods for dynamic single mode operation can also be applied to gratings with second order. In addition, there is one more mechanism not present in lasers with gratings of first order, namely radiation losses. This additional mechanism and the more easy technological access make the grating of second order interesting. Thus in the case of $\pi/2$ phase shift without radiation loss a similarly good yield of aproximately 90 % DSM lasers is achieved as in the case of a laser with radiation losses without phase shift, having at least one facet antireflection coated. The radiation loss method, thus, has specific advantages, but the main disadvantge is, that the

Generally much attention has to be paid to the feedback sensitivity of the DSM/DFB lasers, especially if the frontfacet is antireflection coated and K·L is relatively small.

For 1.5 /um DFB lasers external quantum efficiencies of more than 25 % have been achieved. For a gapmode oscillation by a combination of antireflection coating of the frontside and high reflecting rear side even 38 % have been achieved. The maximum CW output power experimentally determined exceeds 50 mW at 1.5 /um and more than 100 mW at 1.3 /um in DFB lasers. The lowest threshold currents for lasers emitting as 1.5 /um with first order gratings are around 5 mA, L = 100 /um. For lasers with second order gratings and 300 /um length 10 mA have been achieved. In both cases the facets were as cleaved. These values are well comparable regarding the different lengths. Thus, no preference for gratings of first or second order can be derived.

DBR lasers

In a DBR laser the coupling between the active area and the two passive DBR grating areas is an important factor. Thus, threshold currents and internal quantum efficiencies are strongly dependent on the coupling of the active and the two passive waveguides. The two passive waveguides furthermore must have very low losses to achieve a good sidemode suppression ratio. Since the relatively long passive DBR waveguides have a relatively high reflectivity for the Bragg mode the sensitivity against external reflections is lower than in a DFB laser.

The necessity for a low length of the active waveguide has a big disadvantage for the DBR laser: The threshold current densities are much higher than in a DFB laser. This is a disadvantage because the degradation in the system InGaAsP/InP is induced by the current density and not by the optical power as in GaAs. In addition the high threshold current density leads to a high value of the carrier density at threshold, thus, the importance of the Auger effect and intervalence band absorption grows. Also the external quantum efficiency and T_0 drop . For an integration the DBR laser has the additional disadvantage of a relatively great length.

Chirp

DFB lasers as well as DBR lasers have a structure dependent chirp, i.e. the modulation current dependent frequency variation, yielding an envelope curve, which is much broader than the natural laser line. This chirp is, however, many times lower than the dynamical broadening in a Fabry Perot type laser. The dynamical, frequency dependent wavelength shift in both types is comparable and can be minimized by the choice of the structure. Besides that the chirp can be reduced in direct digital modulation by a proper shaping of the current pulses.

Temperature dependence

For an increase of the temperature in a DFB laser the carrier density grows and, thus, the refractive index of the active layer decreases, i.e. the corrugation period optically grows. Hereby the Bragg wavelength moves with increasing temperature in the same direction as the gain curve. This fact makes a big DSM temperature range possible without mode jump (> 100 ^{o}C).

A DBR laser behavious differently since the injection does not take place in the area of the grating. Thus, the optical corrugation period in a DBR laser does not grow by the injection like in a DFB laser. The emission wavelength consequently increases more slowly with increasing temperature than the Bragg wavelength. That means the laserline moves to the short wavelength side with regard to the Bragg wavelength. If this shift is larger than half a mode separation a mode jump occurs. Therefore the maximum temperature range for dynamical single mode operation is larger in a DFB laser as compared to a DBR laser.

Sidemode suppression ratio

Above threshold a nonlinear effect occurs with increasing injection: spatial hole burning. This effect reduces the gain difference between the lasing mode and the next neighbouring mode and in consequence the sidemode suppression ratio. For KL = 1.25 the influence of the nonlinear gain is minimized since under these conditions the photon distribution in the resonator is very flat. The feedback sensitivity under these conditions is, however, high.

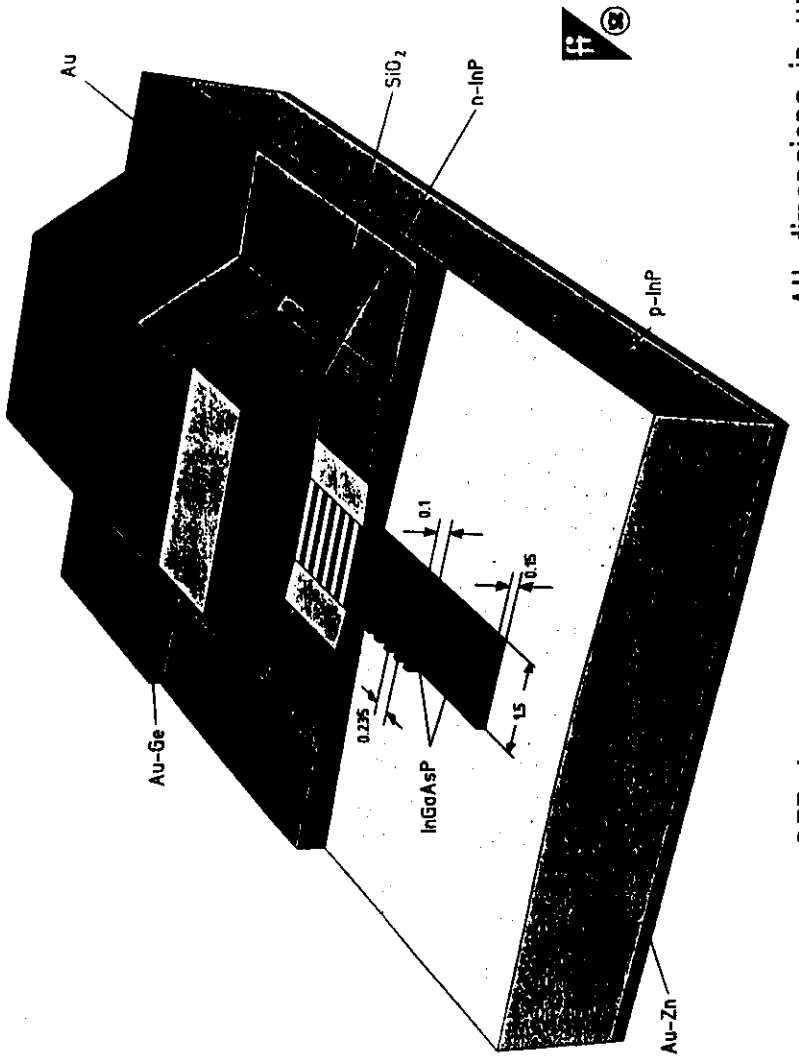

All dimensions in µm

ctional view of a DFB laser

Technological Steps:

1) Epitaxy: LPE or MOVPE

(1.3µm) n InGaAsP	200nm waveguiding layer ($2\cdot10^{17}cm^{-3}$)
(1.53µm) InGaAsP	120 oder 190nm active layer
InP	200nm buffer layer
p-InP substrate	($4\cdot10^{18}cm^{-3}$)

2) definition of grating

Photoluminescence-studies

λ_{PL} + 20nm ⟶ Gain-Maximum = desirable λ_{Laser}

definition of the desirable coupling coefficients K
→ calculation of the grating morphology

amplitude (a = 60-110nm)

distance grating-active layer
(d = 90-100nm)

active layer (b = 120, 190nm)

corrugation period
(Λ = 232.5, 235nm)

duty cycle W/λ

electron beam lithography, Ar/O_2 dry etching (UNI Stgt)

3) regrowth of grating: p-InP ($2\cdot10^{18}cm^{-3}$) MOVPE

4) preparation of the mushroom-stipe structur

a) definition of mesa

N_2^+ dry etching with Ti/Si_3N_4 etch masks

b) under-cutting:

selective etching of
quaternary layers

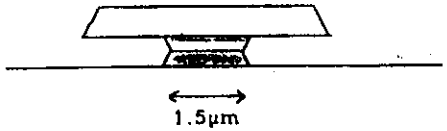

5) rebury of the active layer

- mass transport with intrinsic InP
  or by hydride VPE
- pyrolytic SiO_2-coating

6) etching of wafer to 100 µm residual thickness,
metallic contacts (Au/AuGe/Ni)

7) cleaving into laser diodes of 150-300 µm length

a)

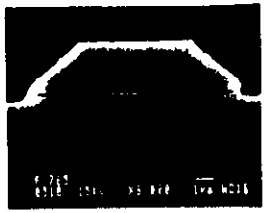

b)

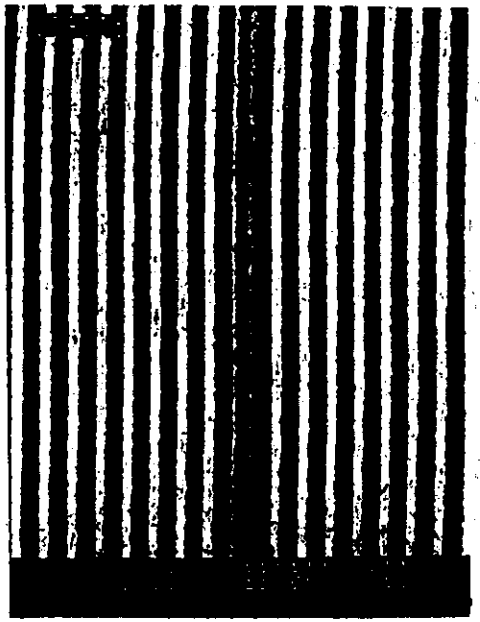

c)

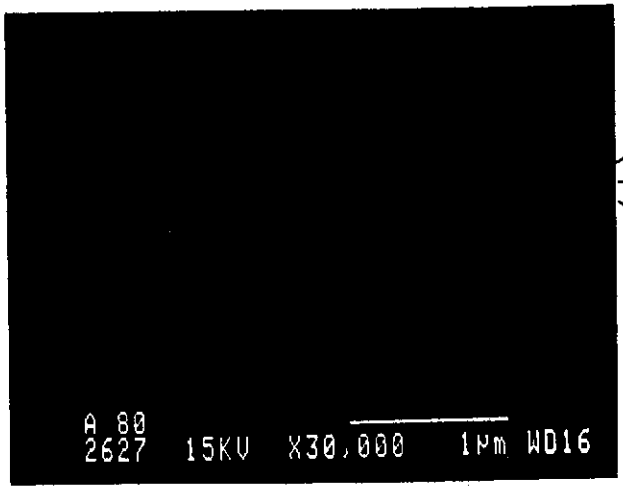

n⁺-InP (n = 10^{18} cm^{-3})

Q (λ = 1.3 µm)

Q (λ = 1.55 µm)

p⁺-InP Substrate
+ buffer (0.2 µm)

DFB Mushroom Laser

a) Cross sectional view
b) 1st order grating with $\lambda/4$-phase shift
c) Layer structure

operties of our strongly coupled DFB laser diodes:

λ_B - 1.52... 1.56 µm

I_{th} - 15 mA (typ. values), lowest values: 9mA

T_o - 60K

$d\lambda/dT$ - 0.08 nm/K

$d\lambda/dI$ - - 0.2 ± 0.05 nm/mA (below threshold)

$d\lambda/dI$ - + 0.011 ± 0.003 nm/mA (above threshold)

SMSR up to 51.2 dB

K - 150 ... 400 cm^{-1} (K·L - 3...9)

η - 0.03 ... 0.18 W/A (depending on the position of phase shift)

chirp - 0.5 nm (at 20dB for 8Gbit/s NRZ)
($I_b - I_{th}$ - 30mA, ΔI_m - 40mA)

eye opening: horiz. - 93%, vert. - 96%

line-widths: 15 MHz without saturation

PRINCIPLES OF WAVEGUIDES

$$\Phi_{ges} = -2dn_1 k\sin\Theta + \varphi_2(n_1,n_2,\Theta) + \varphi_3(n_1,n_3,\Theta)$$
$$= -2m\pi .$$
$$\Phi_x = -2d(n_1 k\sin\Theta)$$

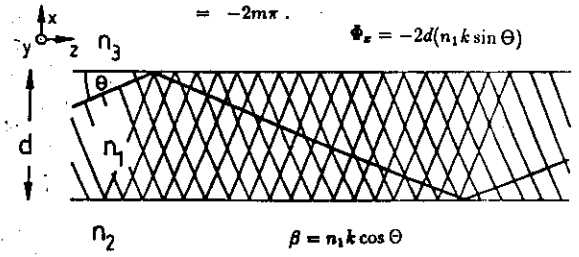

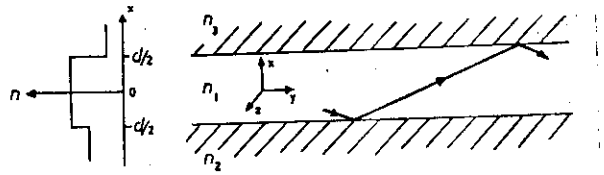

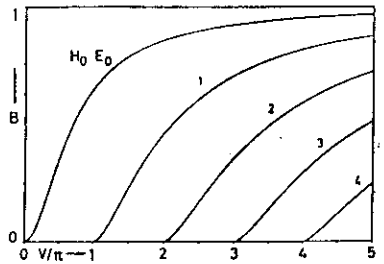

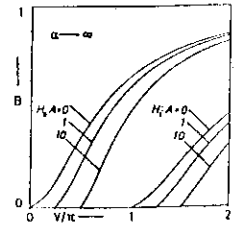

$$B = \frac{\beta^2/k^2 - n_1^2}{n_1^2 - n_2^2}$$

$$V = kd\sqrt{n_1^2 - n_2^2}$$

NORMALIZED PHASE FOR H_p AND E_p-MODES IN A WEAKLY GUIDING, SYMM. (LEFT) AND UNSYMM. (RIGHT) FILM WAVEGUIDE

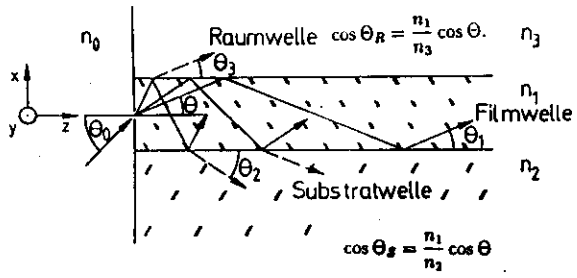

TE:

$$\frac{\partial^2 E}{\partial x^2} + k^2 \{ n^2(x) - n_{eff}^2 \} E = 0$$

$$n_{eff} = 3.3332$$

TM:

$$\frac{\partial^2 H}{\partial x^2} + k^2 \{ n^2(x) - n_{eff}^2 \} H - \frac{1}{n^2}\frac{\partial H}{\partial x}\frac{\partial n^2}{\partial x} = 0$$

$$n_{eff} = 3.3255$$

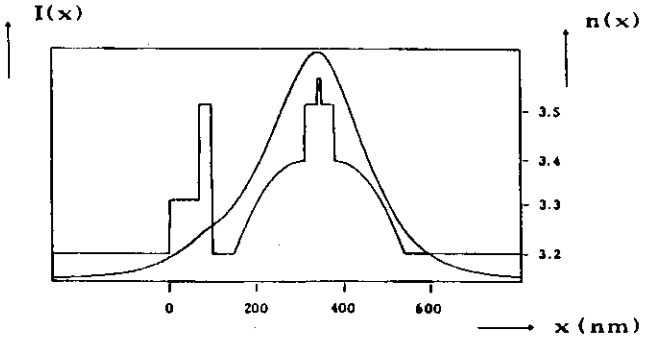

$$n_{eff} = 3.33321$$

COUPLED MODE ANALYSIS

The conventional coupled-mode equations are given by [2], [9]

$$\frac{dA_f^i}{dz} = +(g - j\delta)A_f^i + j\kappa^* A_b^i \quad (1)$$

$$\frac{dA_b^i}{dz} = -(g - j\delta)A_b^i - j\kappa^* A_f^i \quad (2)$$

where

$A_{f(b)}^i = A_{f(b)} \exp -j\beta_{br}\Lambda$ forward (backward) wave
$\beta_{br} = p\pi/\Lambda$ the Bragg wave vector

$\beta_c = \beta_{br} + (\delta + jg) = 2\pi n/\lambda_0$ the traveling wave propagation constant
n = effective refractive index
λ_0 = free-space wavelength
Λ = grating pitch
p = grating order
δ = deviation in propagation constant from Bragg condition
g = electric field amplitude gain
κ = coupling coefficient
* denotes the complex conjugate

$$B_b^i = S_+ B_f^i \text{ (forward eigenmode pair)} \quad (3)$$

$$C_f^i = S_- C_b^i \text{ (backward eigenmode pair)} \quad (4)$$

$$S_+ = \frac{(\delta + jg) \pm [(\delta + jg)^2 - |\kappa|^2]^{1/2}}{\kappa^*} \quad (5)$$

$$S_- = \frac{(\delta + jg) \pm [(\delta + jg)^2 - |\kappa|^2]^{1/2}}{\kappa}. \quad (6)$$

The propagation constant of the eigenmodes (β_c) can be found by assuming

$$A_f^i = A_f'' \exp -j\beta_c z \quad (7)$$

$$A_b^i = A_b'' \exp +j\beta_c z. \quad (8)$$

Substituting (7) and (8) into (1) to (6) results in

$$|\beta_c| = [(\delta + jg)^2 - |\kappa|^2]^{1/2}. \quad (9)$$

We can now write down the forward and backward eigenmode pairs:

forward pair:

$$A_f[\exp -j\beta_{br} z + S_+ \exp +j\beta_{br} z] \exp -j\beta_c z \quad (10)$$

backward pair:

$$A_b[\exp +j\beta_{br} z + S_- \exp -j\beta_{br} z] \exp +j\beta_c z. \quad (11)$$

TRANSFER MATRIX METHOD

PLANE TE-WAVE IN z-DIRECTION : $E_y = E_z = 0$

SINCE $\mathrm{rot}\vec{E} + \dot{\vec{B}} = 0$ AND $\vec{B} \sim e^{j\omega t}$: $E_x = E_x(z)$

$$H_x = H_z = 0 \; ; \quad H_y = -\frac{1}{i\omega\mu_0\mu_r}\frac{\partial E_x}{\partial z} \; ; \; j : \text{Layer number}$$

$$\begin{pmatrix} E_{xj}(z) \\ H_{yj}(z) \end{pmatrix} = \begin{pmatrix} 1 & 1 \\ \beta\tilde{n}_j & -\beta\tilde{n}_j \end{pmatrix}\begin{pmatrix} A_j e^{-ik_j z_j} \\ B_j e^{ik_j z_j} \end{pmatrix}$$

$$= \begin{pmatrix} 1 & 1 \\ \beta\tilde{n}_j & -\beta\tilde{n}_j \end{pmatrix}\begin{pmatrix} E_j^+ \\ E_j^- \end{pmatrix}$$

WHERE : $K_j = \frac{2\pi}{\lambda}(n_j + ik_j) = \frac{\omega}{c}\tilde{n}_j$

$$\beta\tilde{n}_j = \frac{k_j}{\omega\mu_0\mu_r} \approx \tilde{n}_j\sqrt{\frac{\varepsilon_0}{\mu_0}} \quad , \quad \mu_r = 1$$

AT INTERFACE $0 \to 1$, $z = a$:

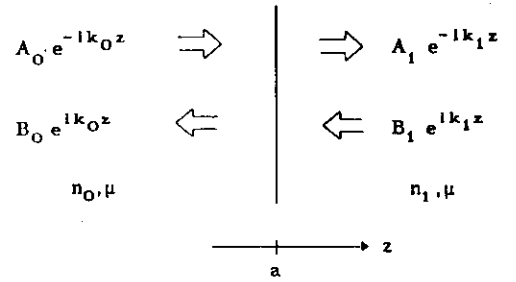

CONTINUITY AT $z = a$ FOR E_z , H_y :

$$A_0 e^{-ik_0 a} + B_0 e^{ik_0 a} = A_1 e^{-ik_1 a} + B_1 e^{ik_1 a}$$

$$i\tilde{n}_0 A_0 e^{-ik_0 a} - i\tilde{n}_0 B_0 e^{ik_0 a} = i\tilde{n}_1 A_1 e^{-ik_1 a} - i\tilde{n}_1 B_1 e^{ik_1 a}$$

RESOLVE FOR A_0 , B_0 :

$$\begin{pmatrix} A_0 \\ B_0 \end{pmatrix} = \begin{pmatrix} \frac{\tilde{n}_0+\tilde{n}_1}{2\tilde{n}_0} e^{i(k_0-k_1)a} & \frac{\tilde{n}_0-\tilde{n}_1}{2\tilde{n}_0} e^{i(k_0+k_1)a} \\ \frac{\tilde{n}_0-\tilde{n}_1}{2\tilde{n}_0} e^{-i(k_0+k_1)a} & \frac{\tilde{n}_0+\tilde{n}_1}{2\tilde{n}_0} e^{-i(k_0-k_1)a} \end{pmatrix}\begin{pmatrix} A_1 \\ B_1 \end{pmatrix}$$

OR : E_0^+ , E_0^- :

$$\begin{pmatrix} E_0^+(z=a) \\ E_0^-(z=a) \end{pmatrix} = \begin{pmatrix} \frac{\tilde{n}_0+\tilde{n}_1}{2\tilde{n}_0} & \frac{\tilde{n}_0-\tilde{n}_1}{2\tilde{n}_0} \\ \frac{\tilde{n}_0-\tilde{n}_1}{2\tilde{n}_0} & \frac{\tilde{n}_0+\tilde{n}_1}{2\tilde{n}_0} \end{pmatrix}\begin{pmatrix} E_1^+(z=a) \\ E_1^-(z=a) \end{pmatrix}$$

FOR A HOMOGENEOUS LAYER :

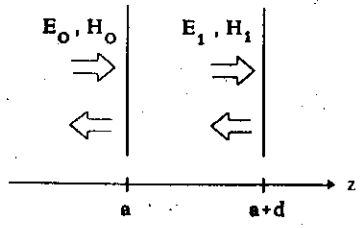

$E_0 \equiv E_{Ges.}(z=a)$

$E_1 \equiv E_{Ges.}(z=a+d)$

$$\begin{pmatrix} E_0 \\ H_0 \end{pmatrix} = \begin{pmatrix} 1 & 1 \\ \beta\tilde{n}_0 & -\beta\tilde{n}_0 \end{pmatrix}\begin{pmatrix} E_0^+(z=a) \\ E_0^-(z=a) \end{pmatrix}$$

$$= \begin{pmatrix} 1 & 1 \\ \beta\tilde{n}_0 & -\beta\tilde{n}_0 \end{pmatrix}\begin{pmatrix} \frac{\tilde{n}_0+\tilde{n}_1}{2\tilde{n}_0} & \frac{\tilde{n}_0-\tilde{n}_1}{2\tilde{n}_0} \\ \frac{\tilde{n}_0-\tilde{n}_1}{2\tilde{n}_0} & \frac{\tilde{n}_0+\tilde{n}_1}{2\tilde{n}_0} \end{pmatrix}\begin{pmatrix} e^{ik_1 d} & \\ & e^{-ik_1 d} \end{pmatrix}\begin{pmatrix} 1 & 1 \\ \beta\tilde{n}_1 & -\beta\tilde{n}_1 \end{pmatrix}^{-1}\begin{pmatrix} E_1 \\ H_1 \end{pmatrix}$$

$$= \begin{pmatrix} \cos k_1 d & \frac{1}{\beta\tilde{n}_1}\sin k_1 d \\ i\beta\tilde{n}_1 \sin k_1 d & \cos k_1 d \end{pmatrix}\begin{pmatrix} E_1 \\ H_1 \end{pmatrix} \equiv \mathbf{M}_1 \begin{pmatrix} E_1 \\ H_1 \end{pmatrix}$$

UPON INVERSION WE YIELD :

$$\begin{pmatrix} E_1 \\ H_1 \end{pmatrix} = \begin{pmatrix} \cos k_1 d & -\frac{i}{\beta\tilde{n}_1}\sin k_1 d \end{pmatrix}\begin{pmatrix} E_0 \end{pmatrix}$$

MULTI LAYER. STRUCTURES

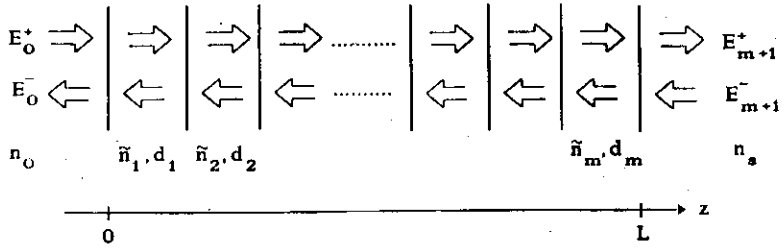

$$\begin{pmatrix} E_0 \\ H_0 \end{pmatrix} = M_1 \begin{pmatrix} E_1 \\ H_1 \end{pmatrix} = M_1 M_2 \begin{pmatrix} E_2 \\ H_2 \end{pmatrix} = \prod_{j=1..m} M_j \begin{pmatrix} E_m \\ H_m \end{pmatrix}$$

THE REFLECTION AND TRANSMISSION COEFFICIENTS ARE:

$$R \equiv \frac{I_r}{I_e} = \frac{|E_0^-|^2}{|E_0^+|^2} = \frac{\left| E_0 - \frac{H_0}{\beta n_0} \right|^2}{\left| E_0 + \frac{H_0}{\beta n_0} \right|^2}$$

$$T \equiv \frac{I_t}{I_e} = \frac{n_s}{n_0} \frac{|E_{m+1}^+|^2}{|E_0^+|^2} = \frac{n_s}{n_0} \frac{|E_m|^2}{|E_0^+|^2} = \frac{4 n_s n_0}{\left| E_0 n_0 + \frac{H_0}{\beta} \right|^2}$$

R, T :

THE RESULT OF THE MATRIX MULTIPLICATION IS A COMPLEX MATRIX M ; SEPARATION INTO REAL- AND IM.PAR

$$\underline{M} = \underline{R} + i\,\underline{I} = \begin{pmatrix} R_{11} & R_{12} \\ R_{21} & R_{22} \end{pmatrix} + i \begin{pmatrix} I_{11} & I_{12} \\ I_{21} & I_{22} \end{pmatrix}$$

$$E_m = 1 \longrightarrow H_m = \beta n_s$$

$$\begin{pmatrix} E_0 \\ H_0 \end{pmatrix} = M \begin{pmatrix} 1 \\ \beta n_s \end{pmatrix}$$

$$T = \frac{4 n_s n_0}{\left| E_0 n_0 + \frac{H_0}{\beta} \right|^2} = \frac{4 n_s n_0}{\left| (M_{11} + M_{12}\beta n_s) n_0 + (M_{21} + M_{22}\beta n_s) n_0 \right|^2}$$

$$= \frac{4 n_s n_0}{\left\{ (R_{11} + R_{12}\beta n_s) n_0 + R_{21} + R_{22}\beta n_s \right\}^2 + \left\{ (I_{11} + I_{12}\beta n_s) n_0 + I_{21} + I_{22}\beta n_s \right\}^2}$$

$$R = \frac{\left| E_0 - \frac{H_0}{\beta n_0} \right|^2}{\left| E_0 + \frac{H_0}{\beta n_0} \right|^2} = \frac{\left| (M_{11} - M_{12}\beta n_s) n_0 + (M_{21} - M_{22}\beta n_s) n_0 \right|^2}{\left| (M_{11} + M_{12}\beta n_s) n_0 + (M_{21} + M_{22}\beta n_s) n_0 \right|^2}$$

$$= \frac{\left\{ (R_{11} - R_{12}\beta n_s) n_0 + R_{21} - R_{22}\beta n_s \right\}^2 + \left\{ (I_{11} - I_{12}\beta n_s) n_0 + I_{21} - I_{22}\beta n_s \right\}^2}{\left\{ (R_{11} + R_{12}\beta n_s) n_0 + R_{21} + R_{22}\beta n_s \right\}^2 + \left\{ (I_{11} + I_{12}\beta n_s) n_0 + I_{21} + I_{22}\beta n_s \right\}^2}$$

THRESHOLD CONDITION FOR AN UNSYMMETRICAL LASER STRUCTURE :

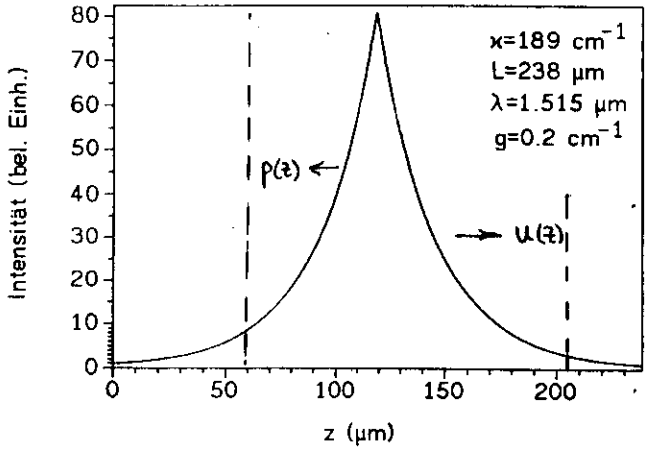

T_0 T_L

$u(z)$ DENSITY OF PHOTONS TO THE RIGHT $\sim |E^+|^2$

$p(z)$ " " " LEFT $\sim |E^-|^2$

T FACET TRANSMISSION

THRESHOLD : GAIN ≡ LOSSES

LOSSES : $T_0\, p(0) + T_L\, u(L)$

GAIN : $du = u(z) \cdot g(z)\, dz$

$$u = \int_0^L g(z)\, u(z)\, dz$$

$g(z)$ CONST. : $\text{GAIN} = g \int_0^L u(z)\,dz + g \int_0^L p(z)\,dz$

$$\Rightarrow T_0\, p(0) + T_L\, u(L) = \int_0^L g(z) \underbrace{[u(z) + p(z)]}_{I(z)}\, dz$$

$T(p(0) + u(L))$

Determination of the coupling coefficients

1) experimental : from the stopband width:

$$K = \pi\, n_{eff}\, \Delta\lambda_{st} / \lambda_B^2$$

n_{eff} effective refractive index

λ_B bragg-mode wavelength

$\Delta\lambda_{st}$ stopband width

example:

stopband width = 6.6 nm ⟶ **K = 286 cm^{-1}**

coupling coefficients of our DFB laser diodes :

$$K = 150 \ldots 400\ \text{cm}^{-1}$$

$$K \cdot L = 3 \ldots 9$$

2) theoretical :

(I) $K_q = \dfrac{(n_3^2 - n_4^2)}{\lambda_B\, n_{eff}} \Gamma_{corr.} \dfrac{\sin(q\pi W/\Lambda)}{q}$ (Streifer et al.

(II) $K_q = \dfrac{\pi}{\lambda_B} \cdot \dfrac{dn_{eff}}{d(d)} \cdot a \cdot F_q$ (Benoit et al.)

rectangle : $F_q = \dfrac{2}{\pi} \dfrac{\sin(q\pi W/\Lambda)}{q}$

Spectra taken near threshold :

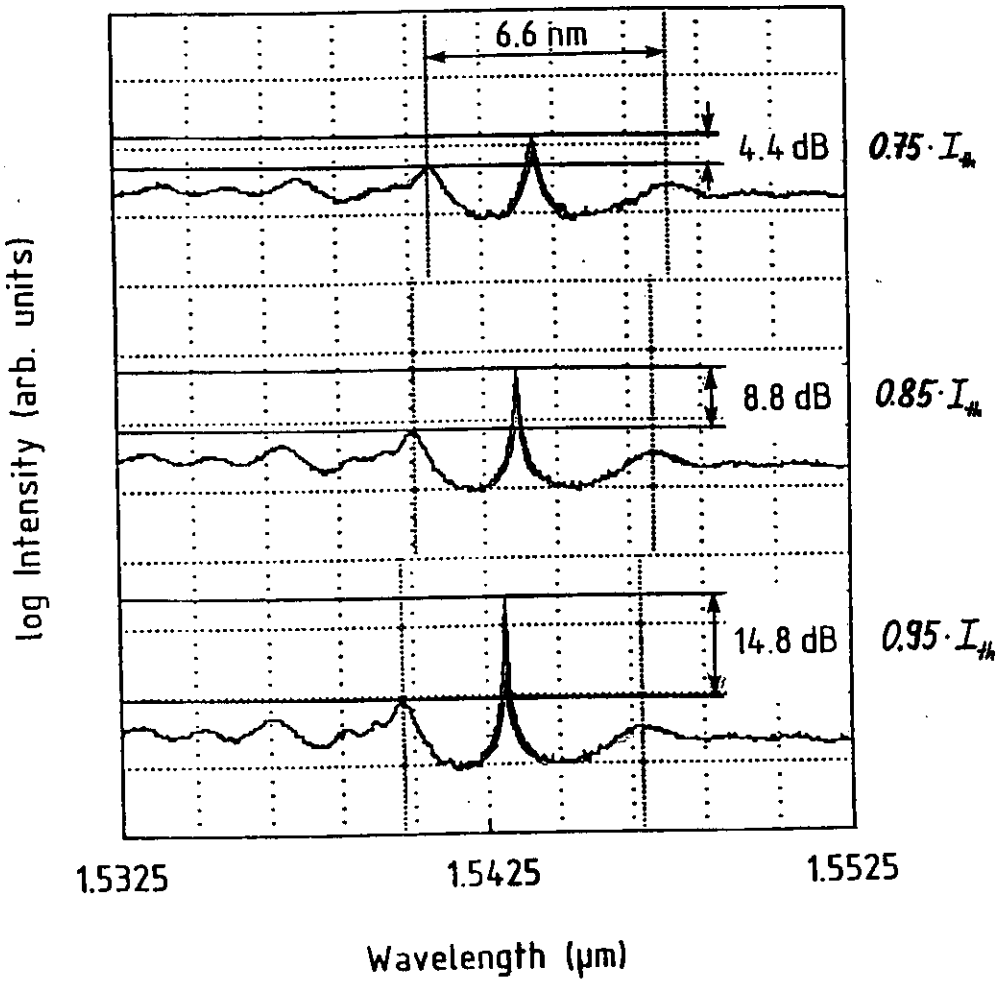

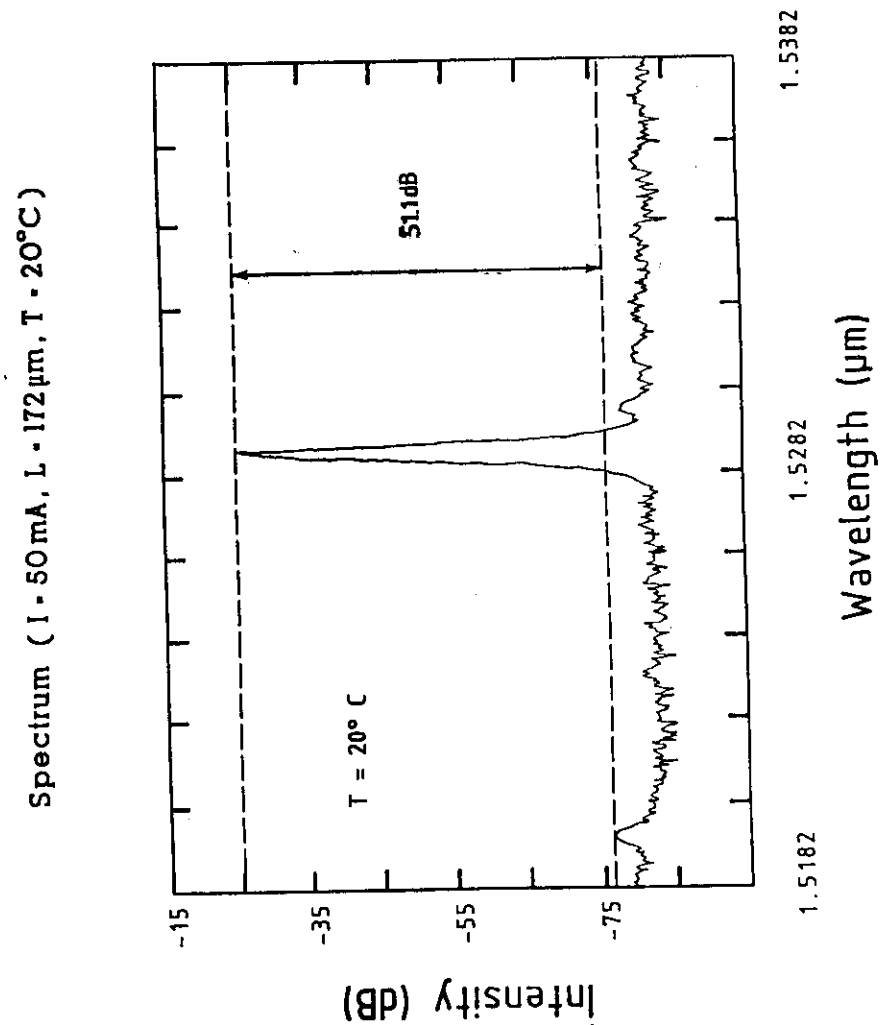

I_{th} ~ typ. 15mA (best values 9mA)

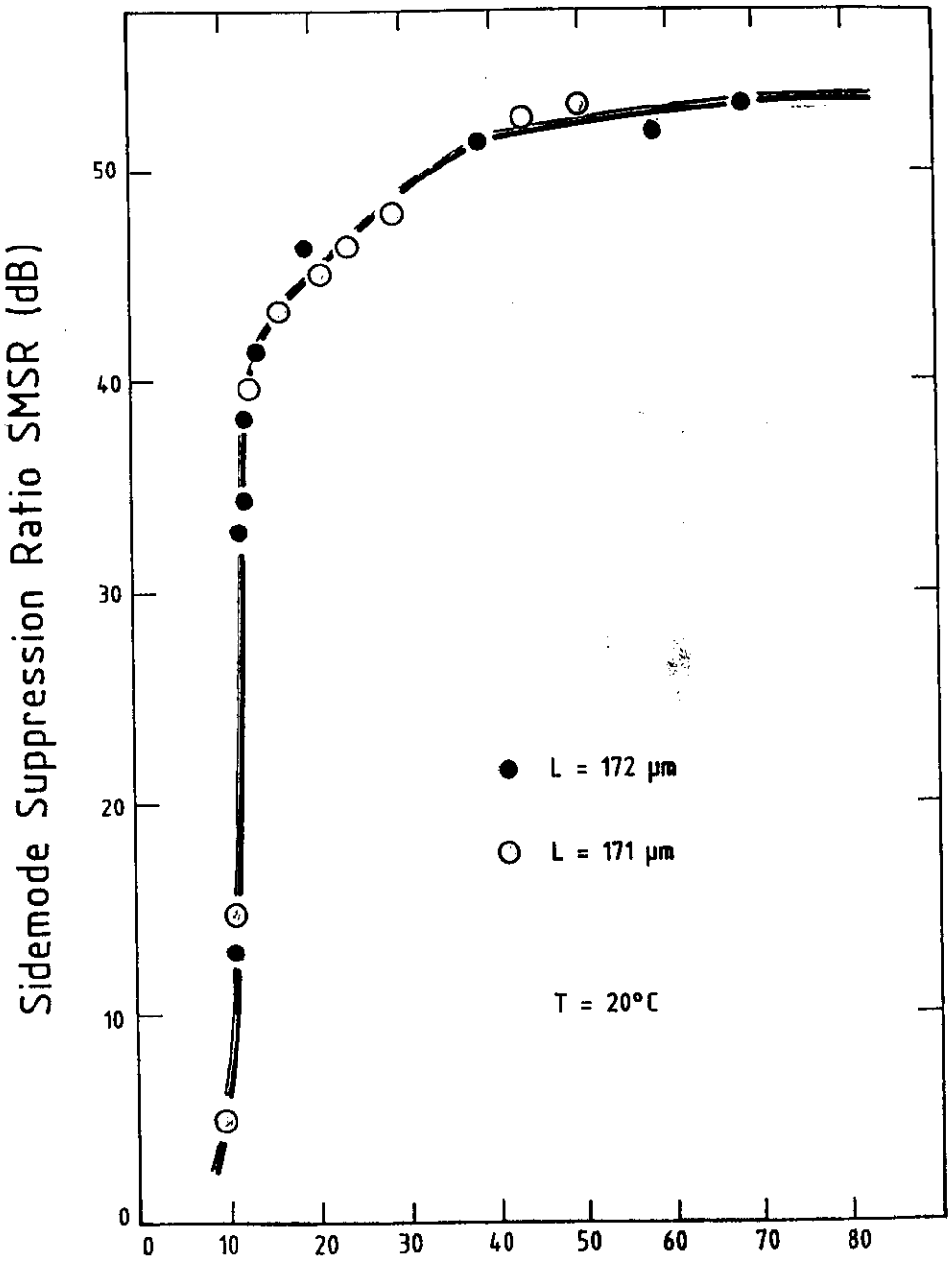

Discussion of high coupling coefficients:

1) reduced sensitivity of the spectra on facet reflectivity

selective etching of facets does not change the main mode oscillation

only 5 – 10% threshold change after $\lambda/4$ Si_3N_4 coating

but $\eta \cdot 0.07 \rightarrow 0.11$ W/A

→ easy handlings for coatings

2) Lower feedback sensitivity

1)
2) due to strong photon pile-up at $\lambda/4$ phase shift

number of photons

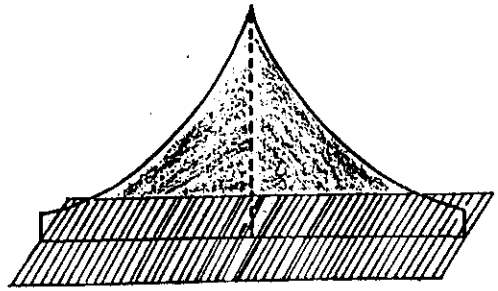

3) However due to high coupling $\eta\downarrow$

can be compensated by placing the $\lambda/4$ phase shift near to the front facet

η - 0.07 W/A ($\lambda/4$ centered)

η - 0.1 W/A ($\lambda/4$ decentered)

best values: η - 0.18 W/A

4) Linewidths: • show no dependence on K·L
• no line width saturation

5) Threshold gain from calculated spectra:

For K·L ≥ 3: bragg mode has the lowest threshold gain compared to the side-modes (independent from the phase of the facet - exact cleaving position in the last corrugation near the facet).

This is not the case for 1 ≤ K·L ≤ 2.

6) No mode jumps as predicted in the literature

7) We even observe enlarged eye-opening in our experiments compared to our simulations based on rate equations for current, photon density, frequency and phase deviation.

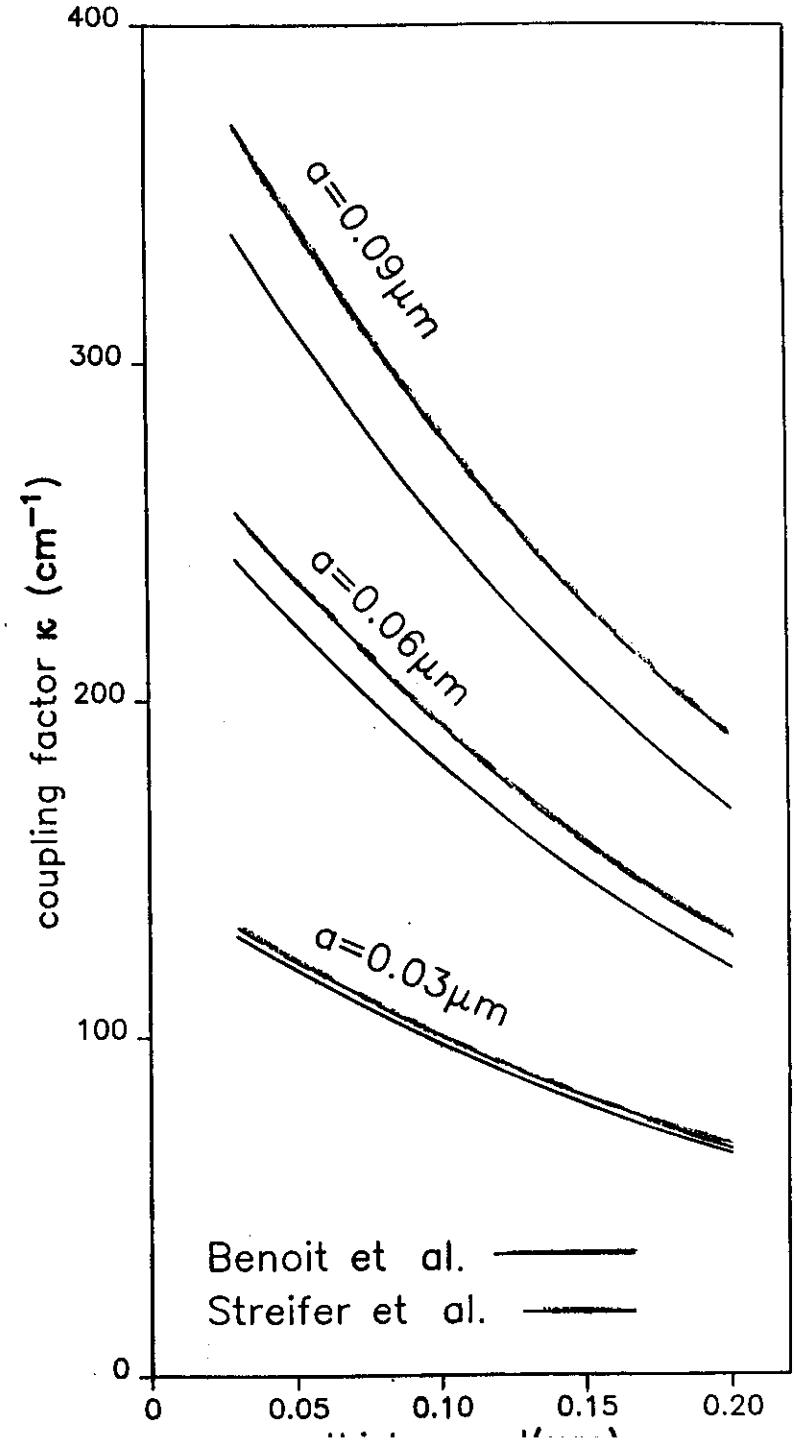

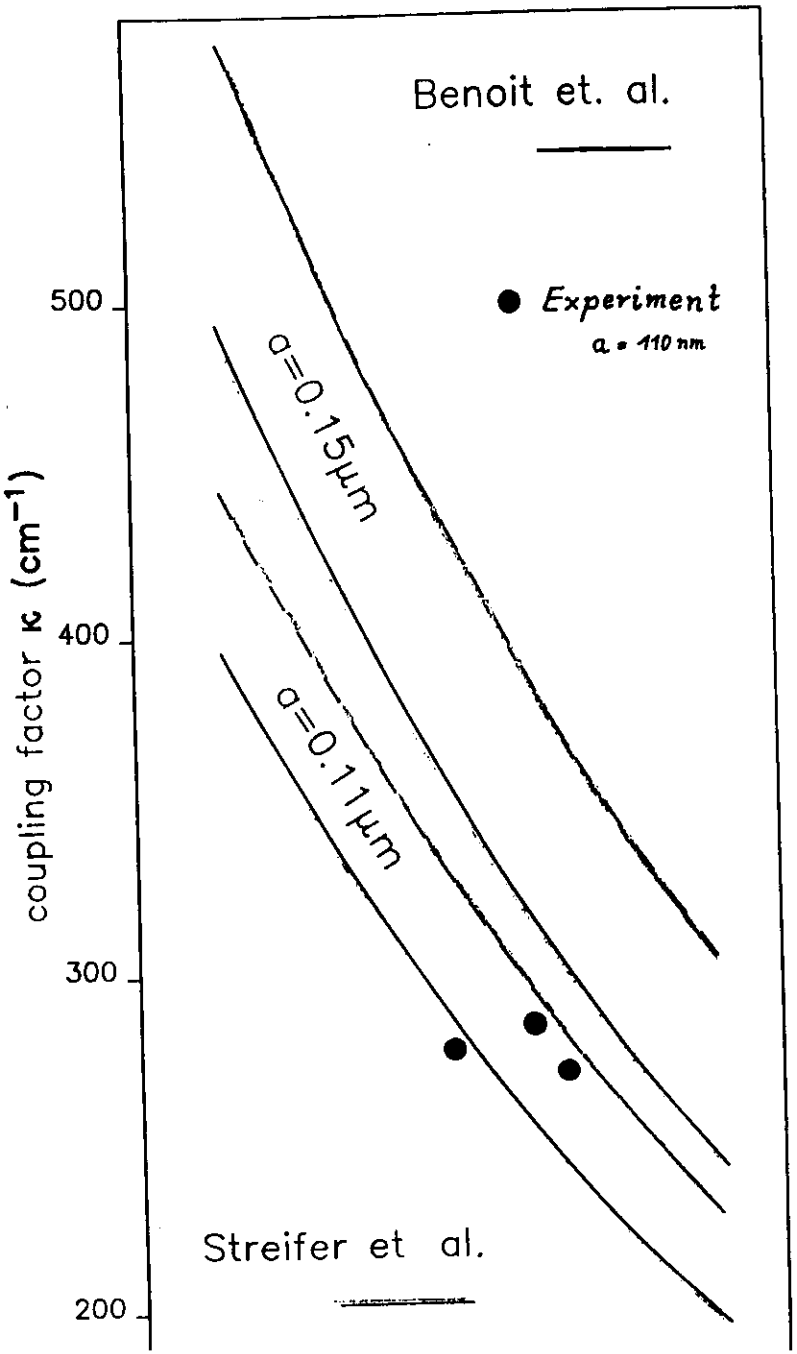

Red/blue shift of the bragg mode

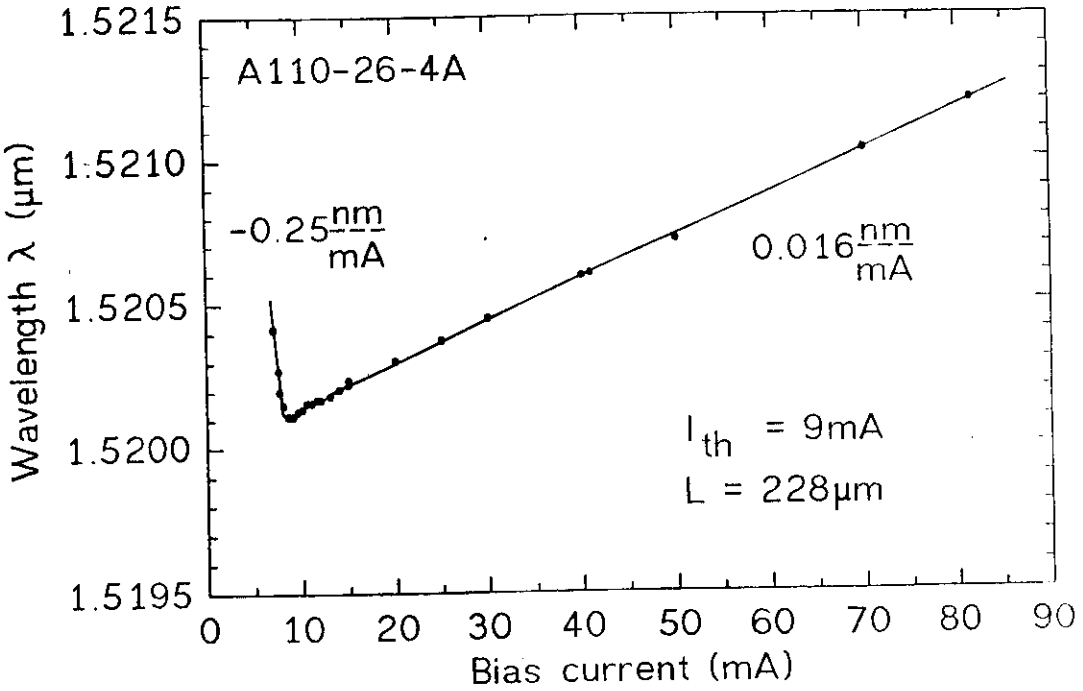

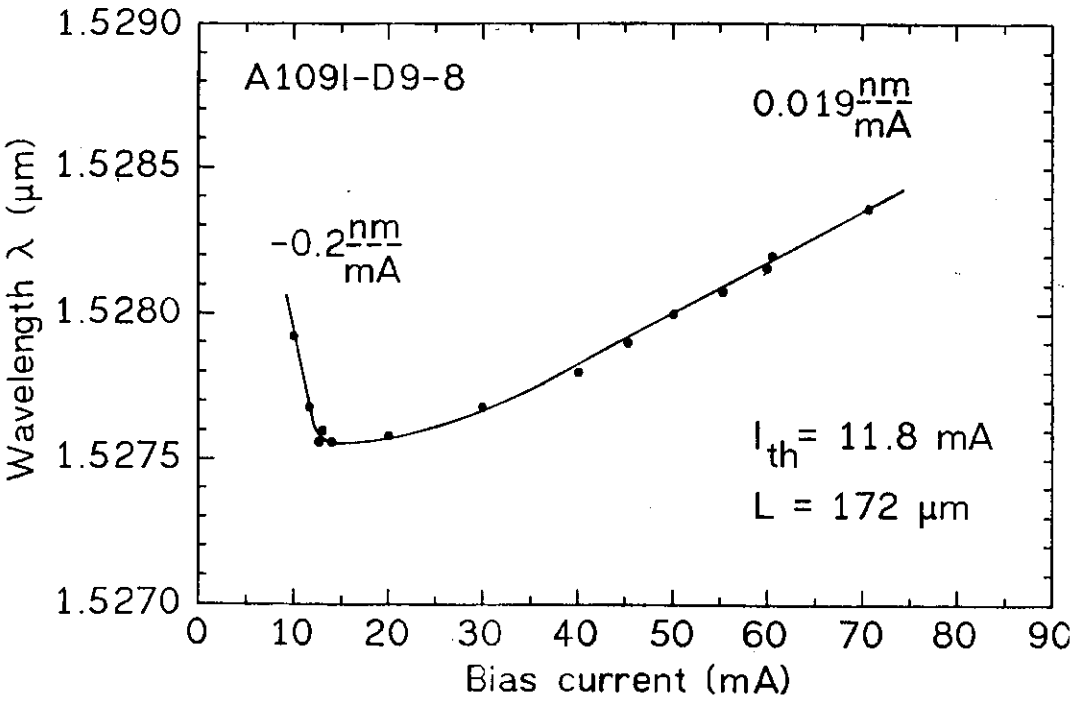

Shift of the bragg-mode wavelength:

$\frac{d\lambda}{dI} > 0$

- band shrinkage due to many-particle effects (high carrier concentrations, band renormalization)
- thermal effects due to high injection currents (Varshni's law).
- gain maximum shifts to higher energies for increasing carrier densities.
- *spatial hole burning*

$\frac{d\lambda}{dI} < 0$

- below and near threshold: refractive index depend sensitively on the energy

(Fermi energy variation, $dn/dN < 0$)

Results for x L - 6

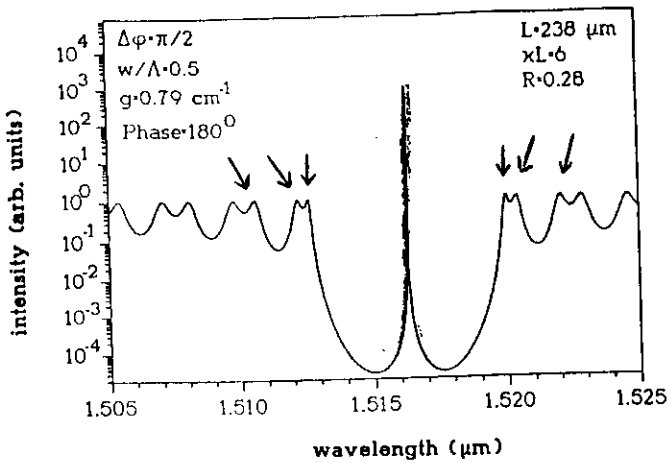

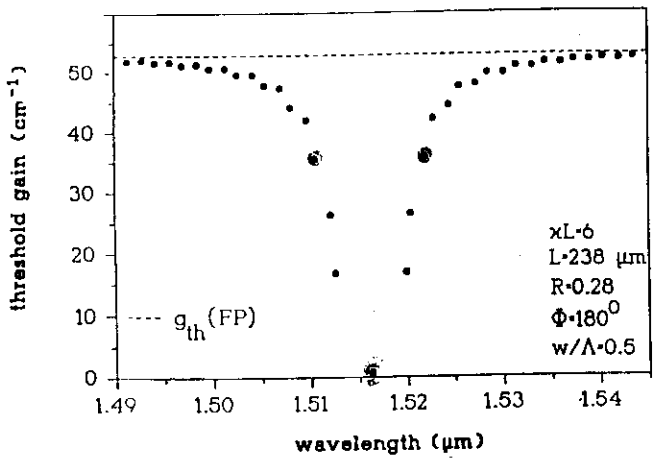

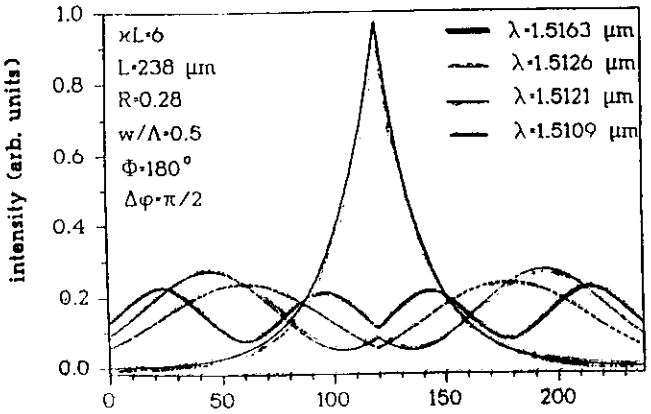

GRATING - PHASE

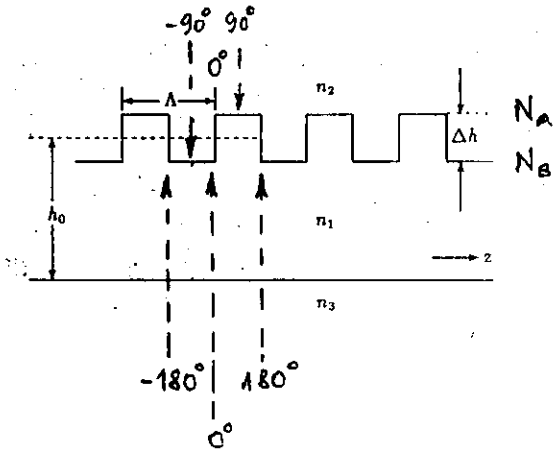

Variation of end-facet phase for xL-6

Definition of end-facet phase Φ :

$$\Phi = 2\pi \frac{d_a N_a}{N_a A + N_b B}$$

Λ = A + B = corrugation period

d = thickness of the outer layers in the laser structure

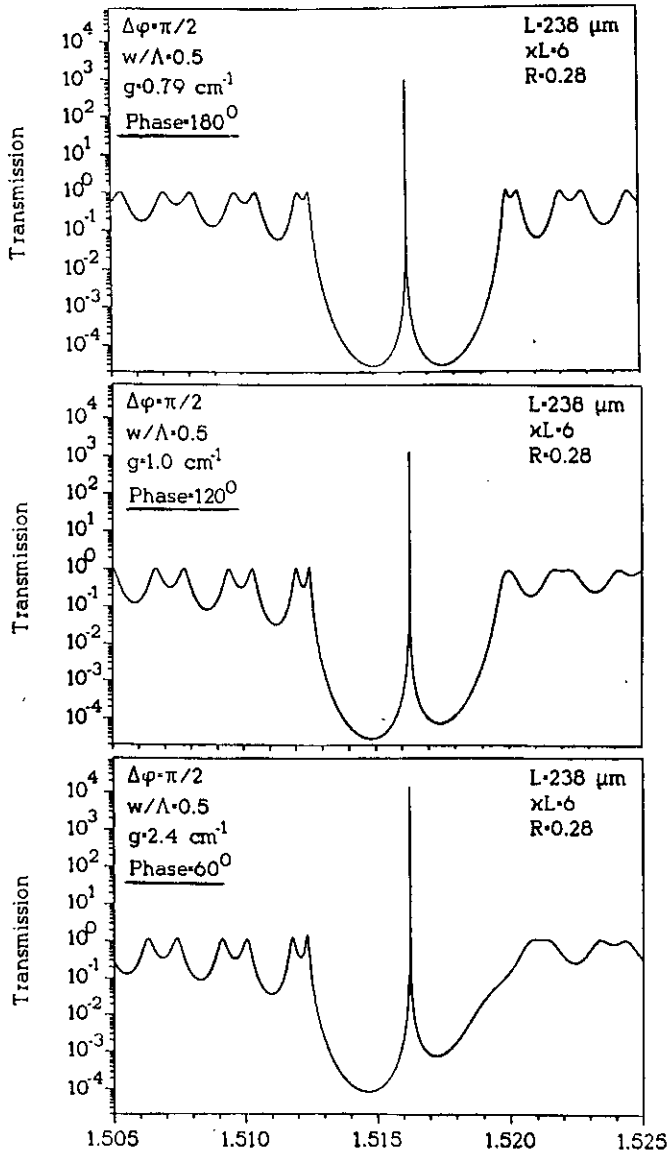

Results for x L - 6

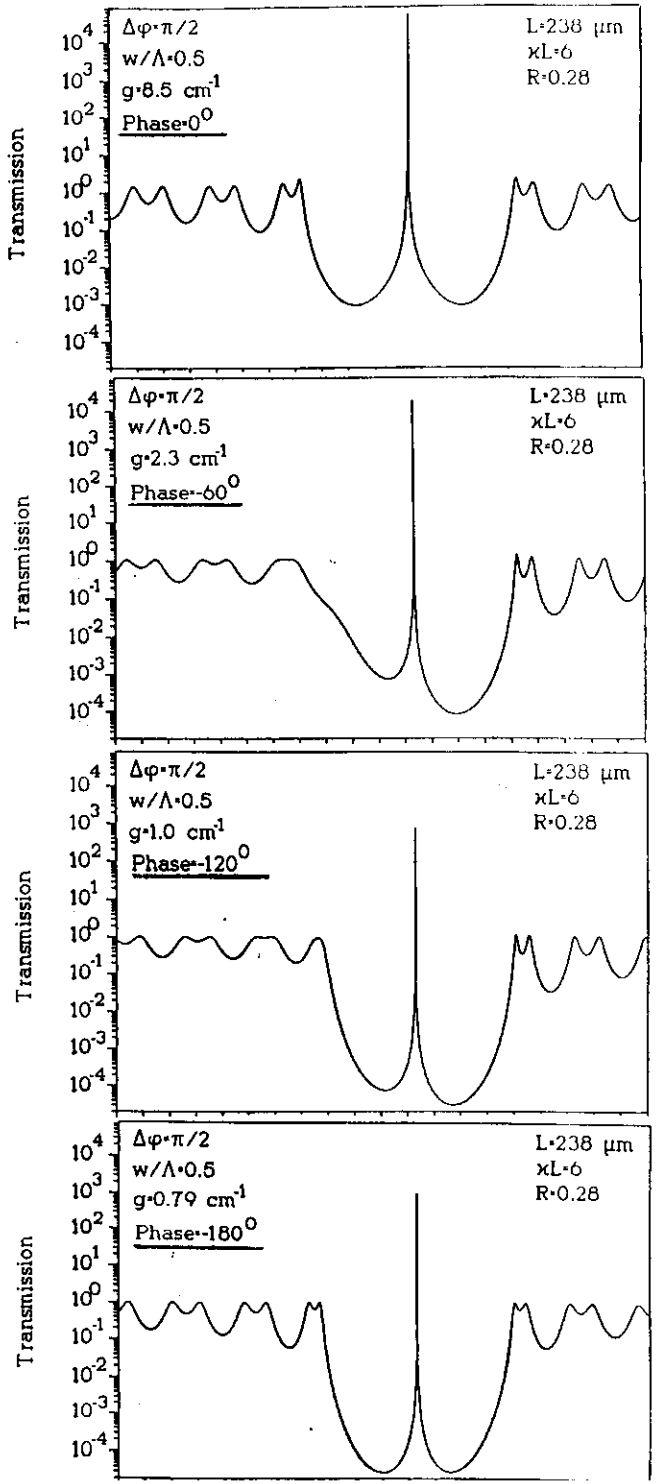

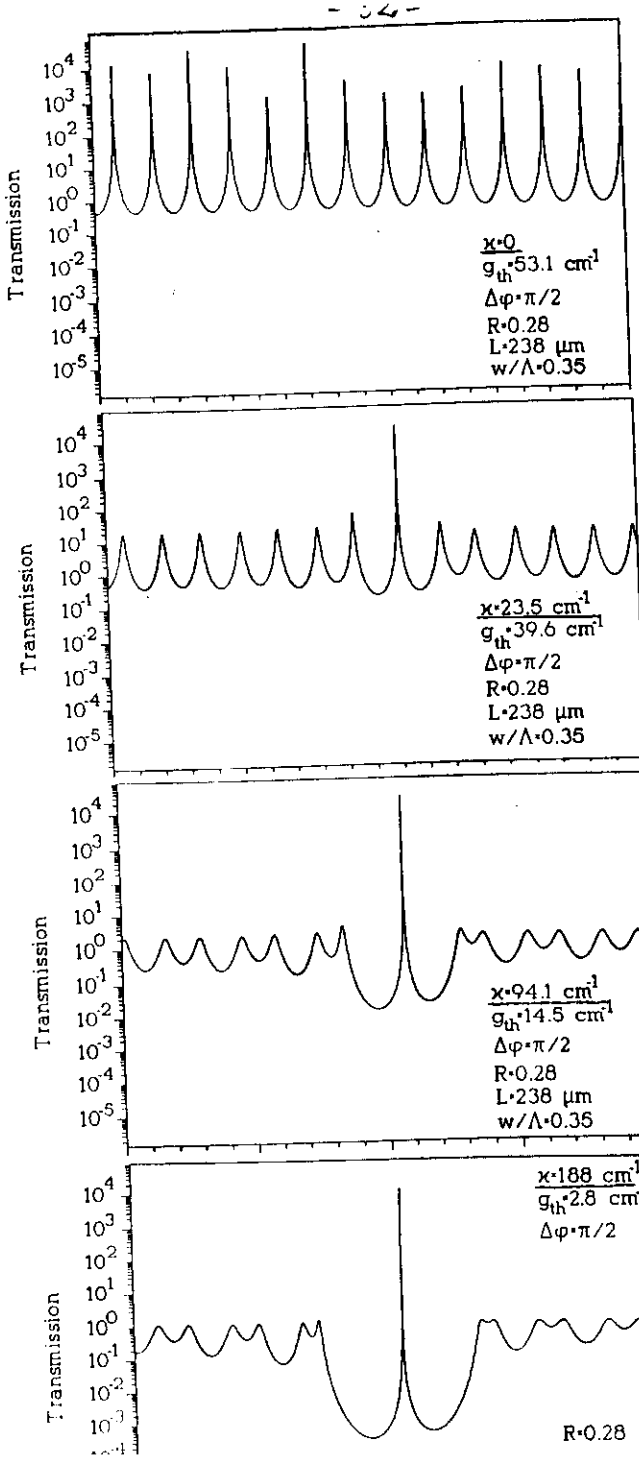

Fabry-perot spectrum

increasing coupling factor →

DFB-spectrum

Sensitivity on end-facet phase

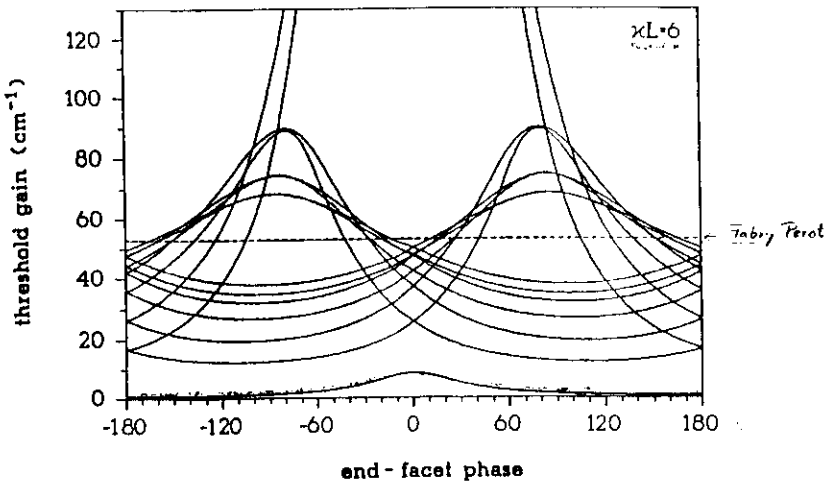

Bragg mode has lowest threshold gain independent of end-facet phase.

Gain difference between Bragg mode and side modes > 15 cm^{-1}

→ **Monomode operation for all values of end-facet phase**

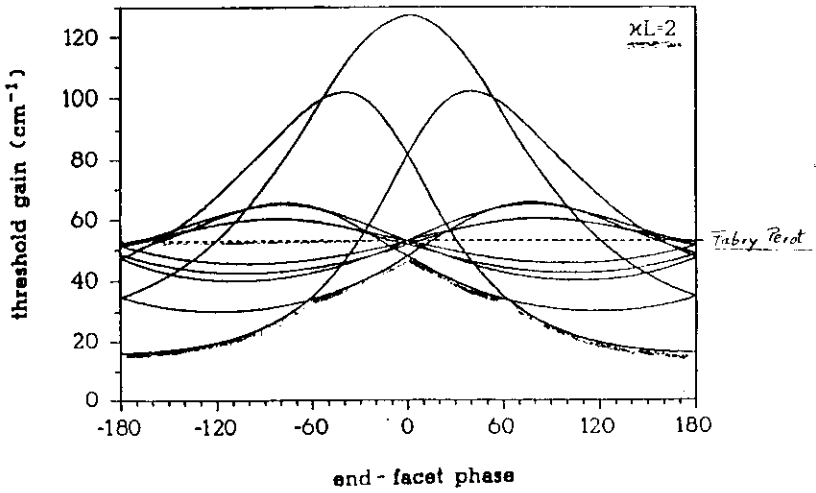

Modal behaviour strongly dependent on exact cleaving position in the last corrugation period near facet

Influences of end-facet phase for κL = 6

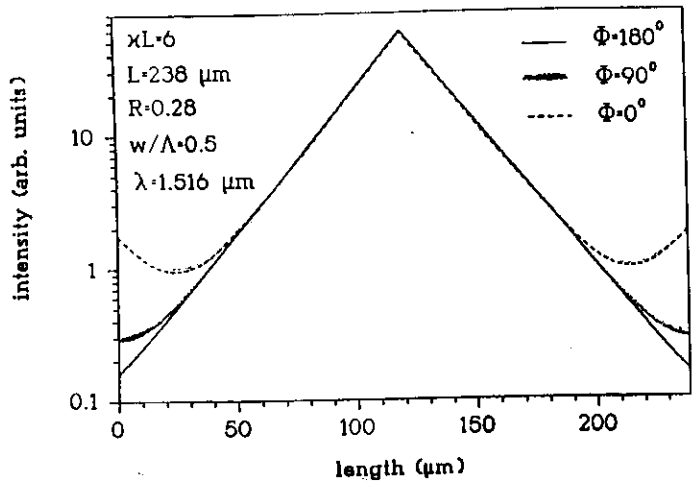

Intensity distribution

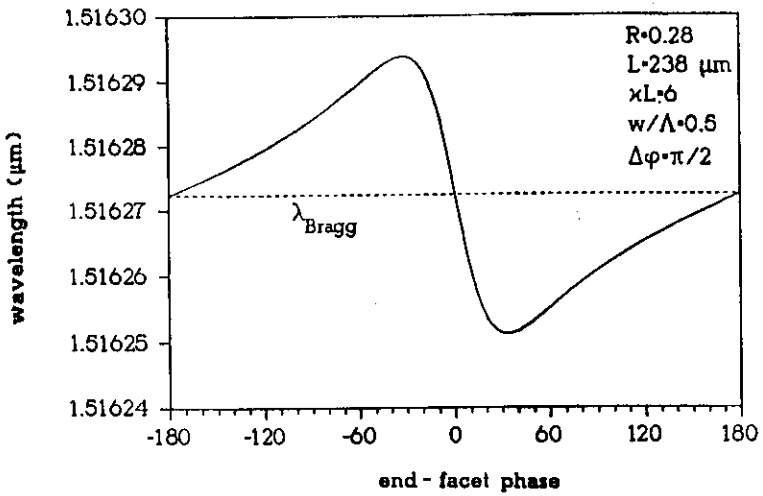

Bragg wavelength

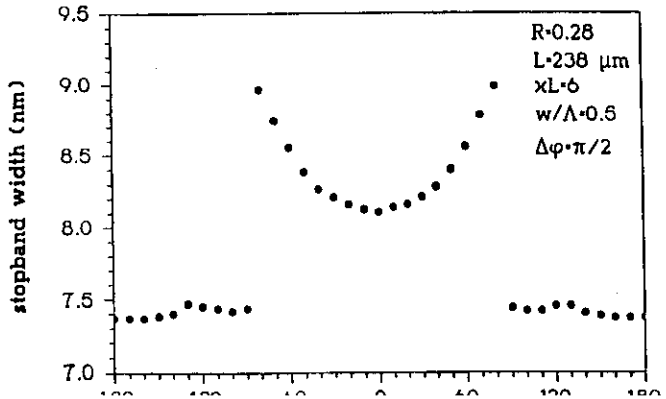

stopband width

Influence of the position and value of the phase shift

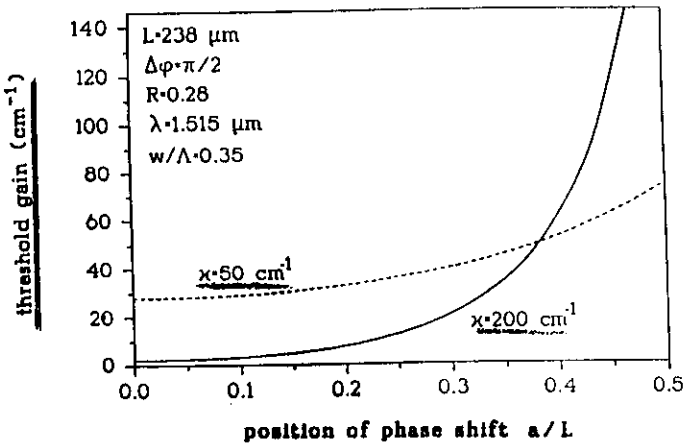

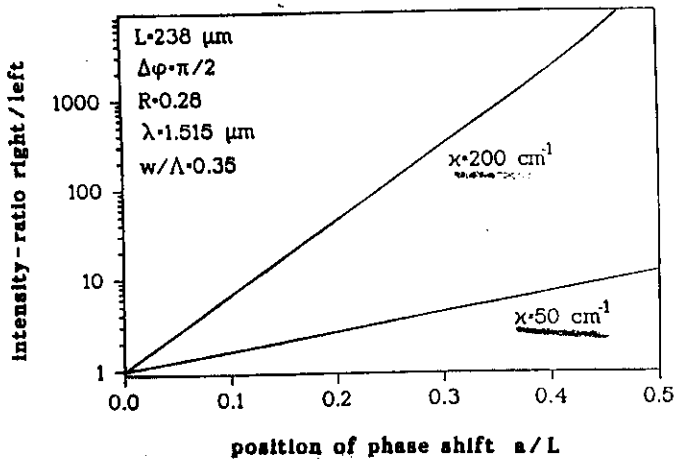

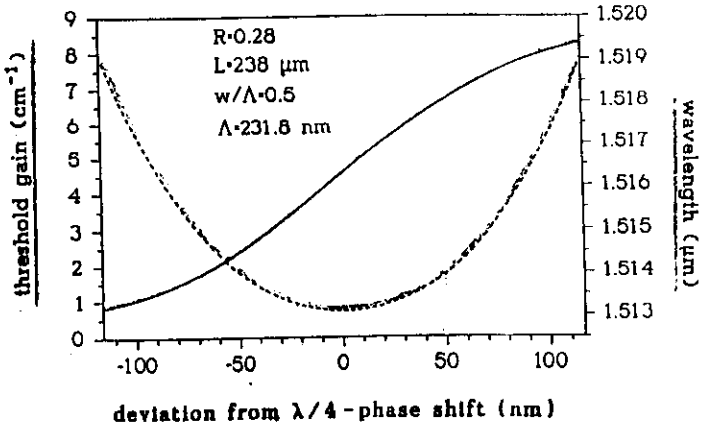

Stopband-width

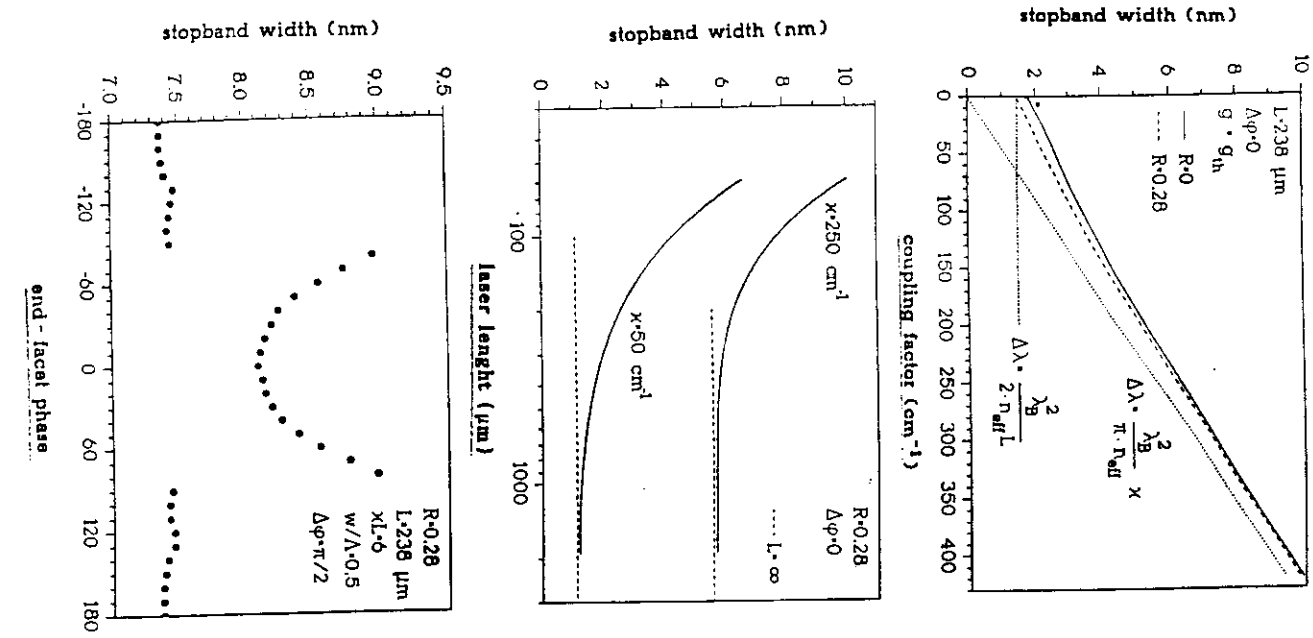

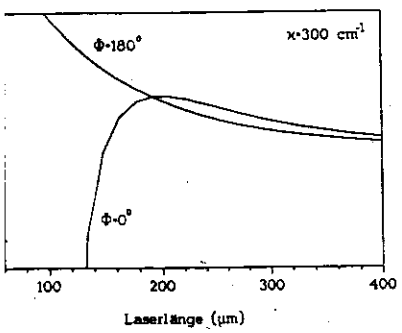

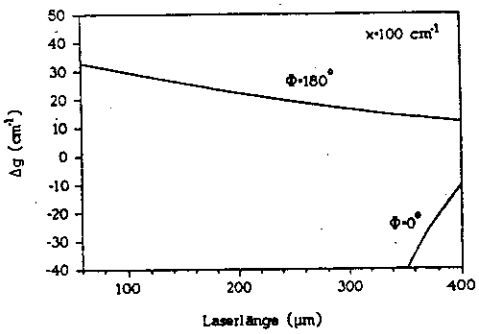

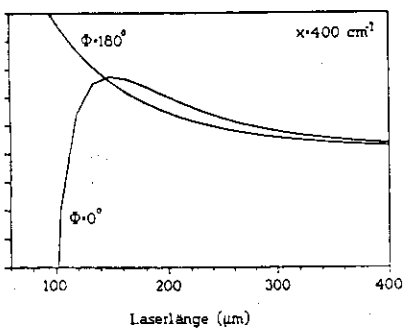

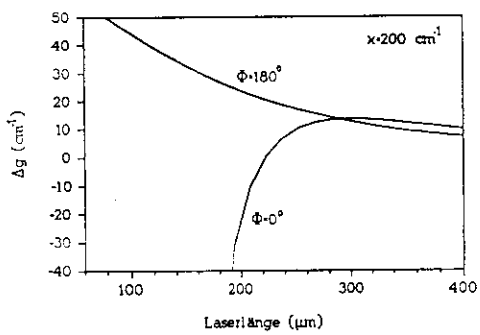

ARIATION OF THRESHOLD GAIN DIFFERENCE BETWEEN BRAGG MODE AND JEXT NEAREST NEIGHBOURING MODE AS A FUNCTION OF THE LASER LENGTH.

AXIALLY VARYING PARAMETERS : SPATIAL HOLE BURNING

RATE EQUATION : n CARRIER DENS. IN ACT. LAYER

$$\frac{dn(z)}{dt} = \frac{I}{eV} - \frac{n(z)}{\tau_e} - \frac{g(n)}{h\nu}\left\{\underbrace{|E^+|^2 + |E^-|^2}_{E^2}\right\}$$

STATIONARY : $\frac{dn}{dt} = 0$; $g(n) = a(n - n_0)$

$|E|^2$ = INTENS. IN ACT. LAYER

$$n(z) = \frac{I/I_0 + |E|^2/P_s}{1 + |E|^2/P_s}\, n_0 \quad ; \quad P_s = \frac{h\nu}{a\tau_e}$$

$$I_0 = \frac{eV}{\tau_e} \cdot n_0$$

$P_s = 0{,}24$ MW/c

$I_0 = 5$ mA

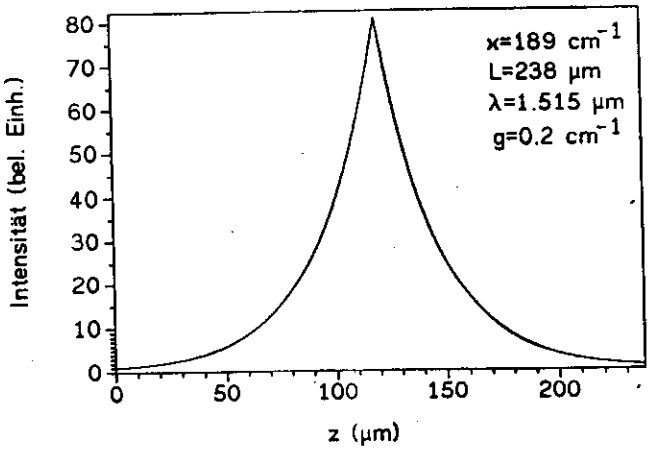

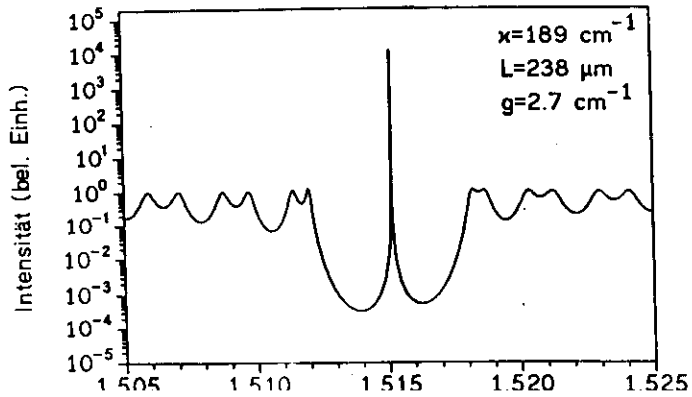

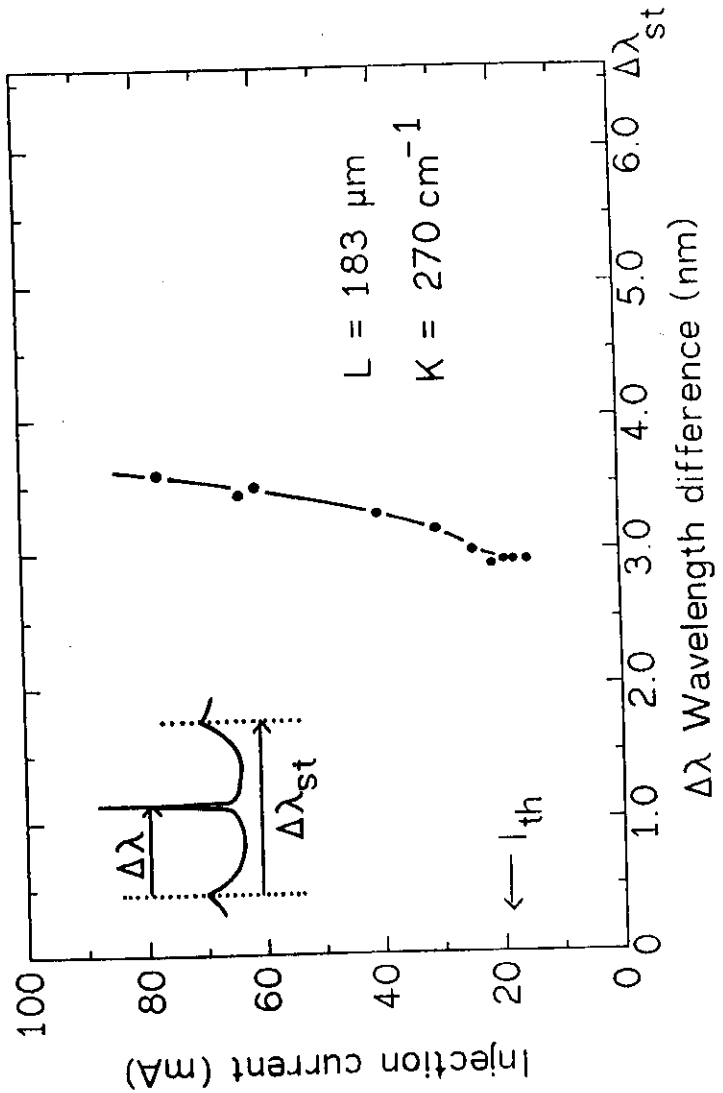

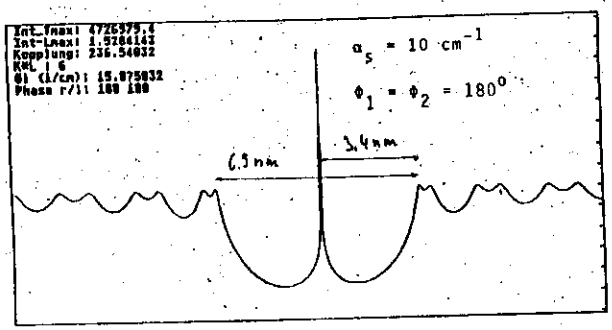

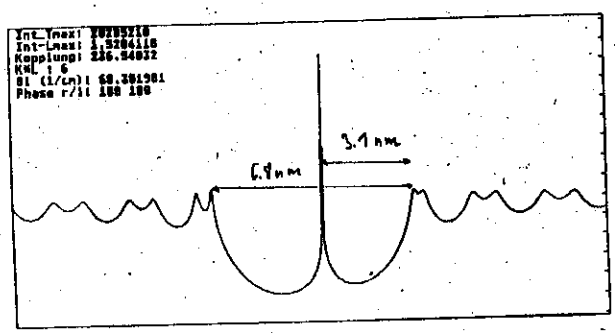

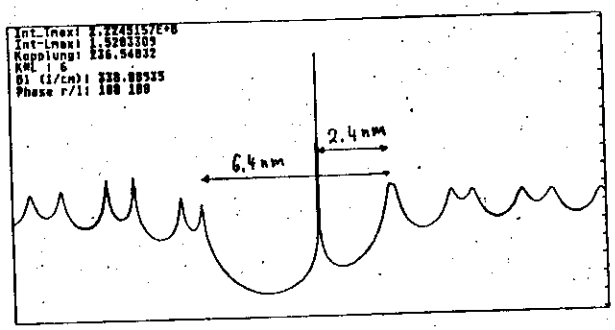

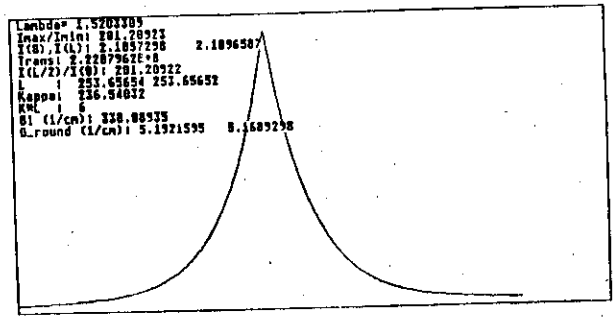

LINEWIDTH :

$$\Delta\nu = \frac{S}{4\pi I}(1+\alpha^2) \qquad \text{(HENRY)}$$

S : spontaneous emission rate for lasing mode

$S = v_g g_{th} n_{sp}$

I : number of photons in cavity (stimul.)

UNSYMMETRICAL PHASE SHIFTED DFB :

$$\Delta\nu = \frac{v_g^2 h\nu\, g_{th}\, n_{sp}\, \alpha_m (1+\alpha^2)}{4\pi (P_1 + P_2)} \; ; \; g_{th} = \alpha_m + \alpha_c$$

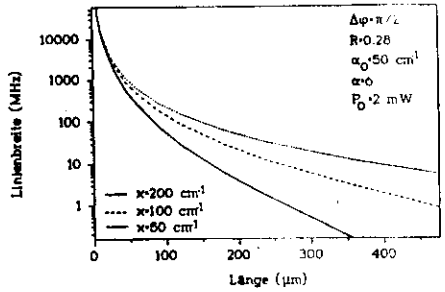

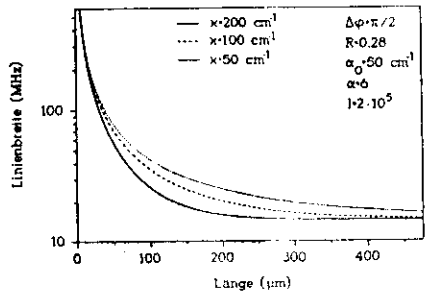

Linewidth measurements

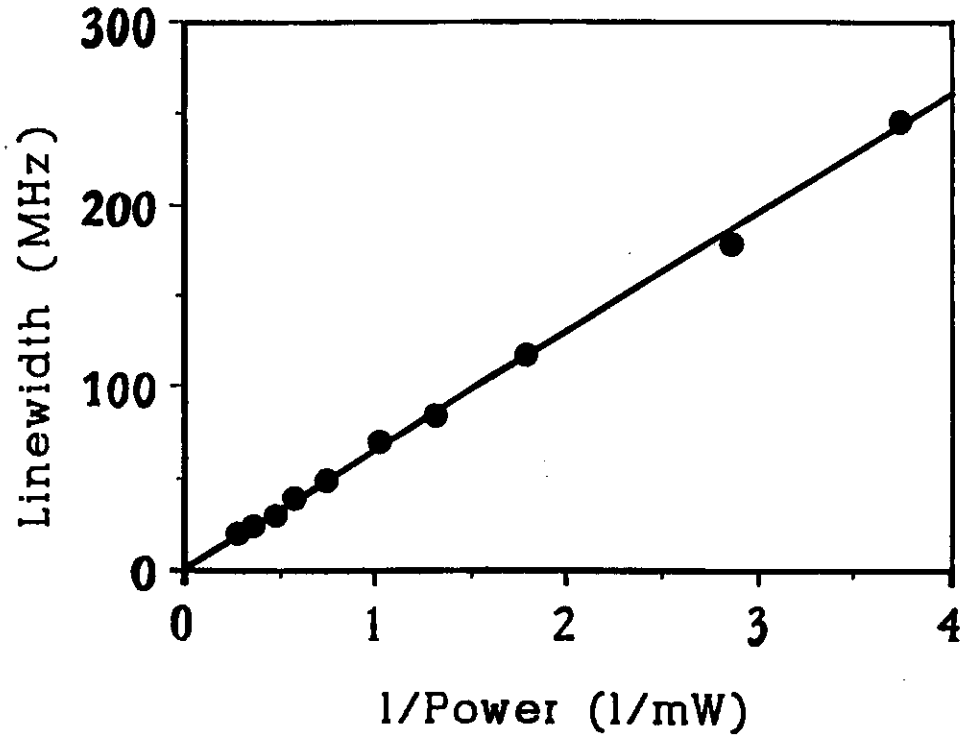

no line width saturation

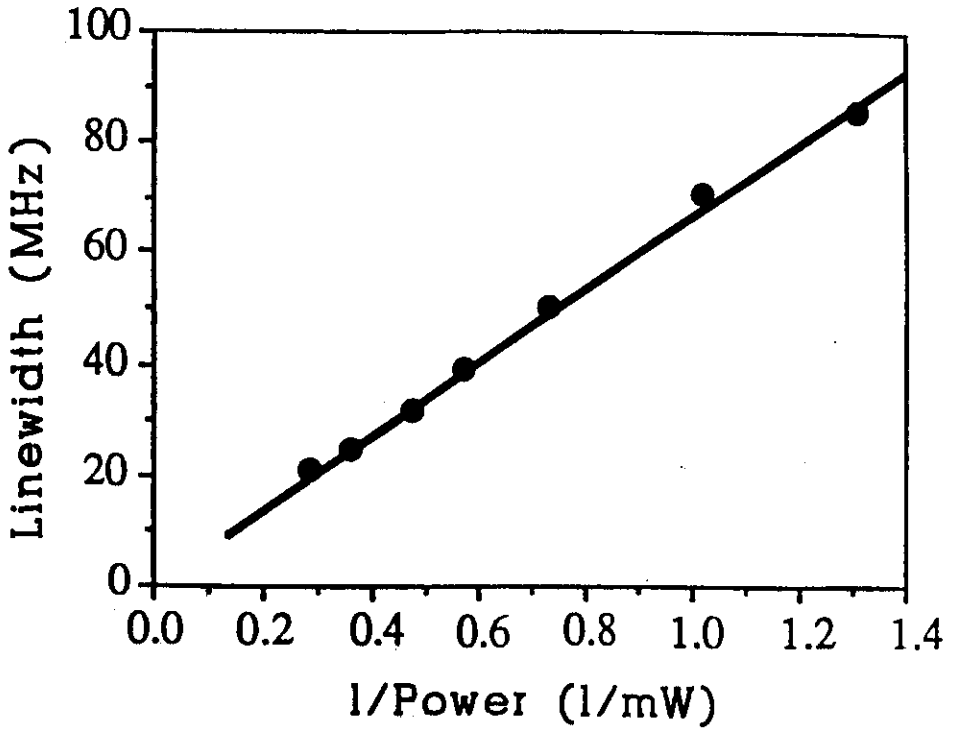

(P. Spano et al.)

Linewidths do not depend strongly on K·L

K·L	4.4	5.7	9
ΔV (MHz)	16	18	22

for a constant K the essential part of the field distribution (photon pile-up) is located on a fixed lenght around the phase-shift independent of L.

linewidth measurements

Optical feedback causes various effects in laser behaviour, especially in laser linewidth. There are five different regions of feedback power ratio (R.W. Tkach & A.R. Chraplyvy; region I ... V). In region I no (external cavity) mode hopping occurs. The emission line is narrowed or broadened, depending on the phase of the feedback light. The more distant the external reflector is, the more sensitive reacts the laser on the feedback. For a very short (~ 1 mm) external resonator mode hopping starts at feedback power ratios increasing above approximately - 50 dB, whereas for a 1.6 m long external cavity the power ratio is about - 80 dB. Thus, very great care has to be taken to prevent linewidth narrowing or broadening or even mode hopping. In region II a rapid mode hopping between external cavity modes occurs for out-of-phase feedback. In the case of in-phase feedback the laser locks to a single mode, resulting in a further reduction of the linewidth. This occurs to the minimum linewidth mode, not the minimum threshold mode (transition I → II). This behaviour ranges up to a feedback power ratio of - 45 dB (independent of the external cavity length) and then changes to region III. Region III is characterized by suppression of mode hopping and single mode oscillation with reduced linewidth as compared to the no-feedback case (no dependence of external cavity length). Region III ranges up to a feedback power ratio of about - 38 dB and then changes to region IV. In region IV satellite modes appear, separated from the main mode by the relaxation oscillation frequency (there is no dependence on external cavity length). These modes increase with increasing feedback, eventually broadening the linewidth to several GHz. This situation has been called "coherence collapse" (coherence length in the order of ~ 1 mm). The transition to this state depends significantly on the α-factor.

In region V the laser operates stably again with a narrow linewidth. This region is usually not to be reached by unintentional feedback. Under normal linewidth measurement conditions one deals with region I or II. The transition from region I to region II may occur at very low feedback levels, depending on the distance of the reflector (- 80 dB for 1.6 m distance). Thus, it is desirable to operate with the first possible reflection very near to the laser (don't use [illegible] fibre pigtails connecting laser and isolator!).

As a rule, one should make the distance laser - first isolator as short as possible with all lens surfaces antireflection coated and eventually tilted. If the sensitivity of the linewidth setup is high enough one can also put the first collimating lens near to the laser and use optical attenuation in the beam to reduce the feedback light level, eg - 20 dB attenuation helps to reduce feedback by - 40 dB.

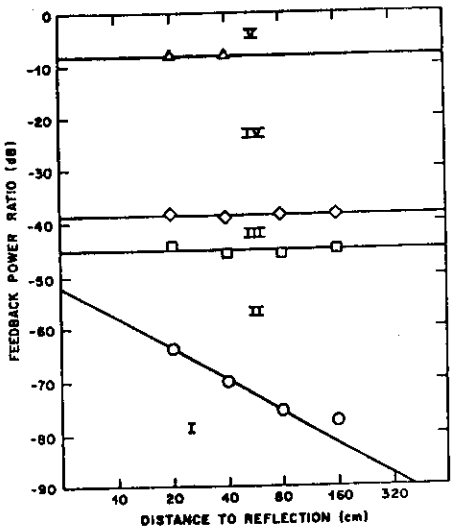

Experimentally observed feedback power levels at which transitions between different regimes of feedback effects occur. The feedback power ratio as defined here corresponds to the effective external mirror reflectivity and the laser was biased well above threshold.

5 Gbit/s NRZ Modulation :

I = 48 mA , ΔI = 40mA

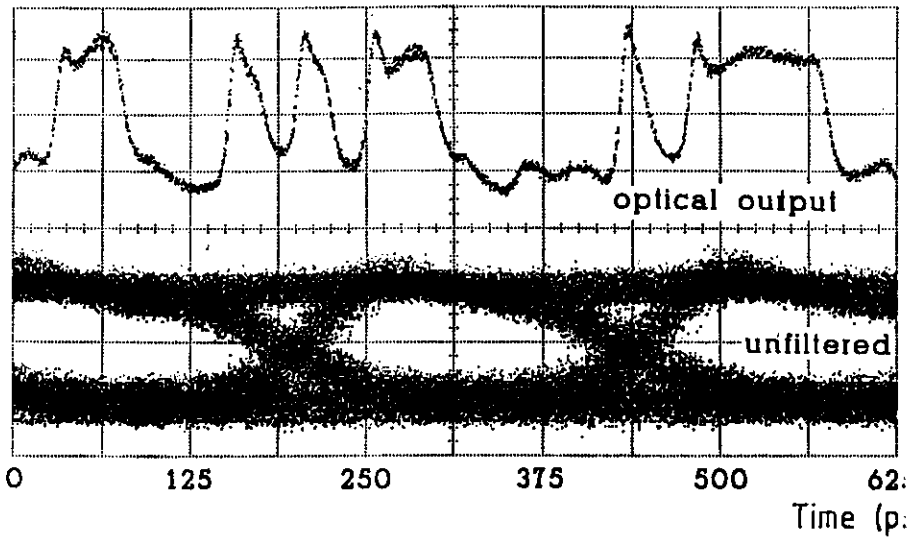

8 Gbit/s NRZ Modulation :

I = 55 mA , ΔI = 40mA

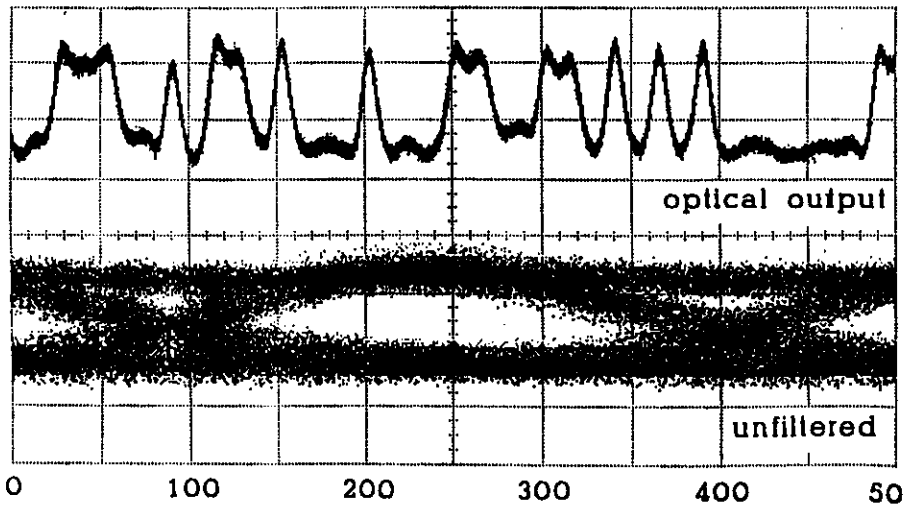

8 Gbit/s NRZ Modulation :

I = 50 mA , ΔI = 40mA

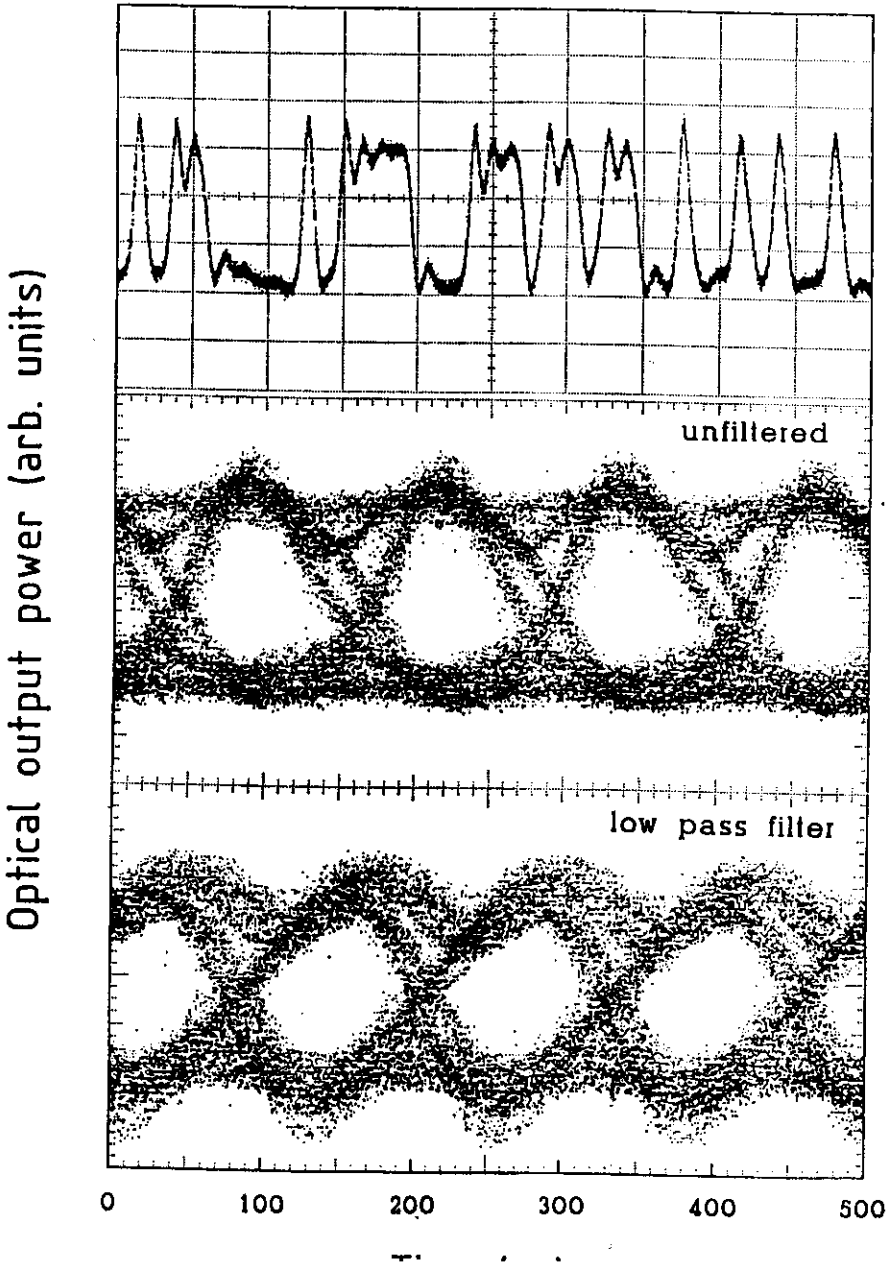

DIRECT DIGITAL MODULATION WITH FEEDBACK

Nr 1 8GHz / 55mA / FP-Typ

(1)

SINGLE-MODE SEMICONDUCTOR LASER WITH EXTERNAL FEEDBACK

ALPHA = 6.00E+00	AN = 2.20E+02	DELTAI = 2.00E-19	DTI = 1.25E-01
IO = 5.50E-19	MYFEXT = 1.00E-09	MYPERI = 1.50E-02	NSP = 2.00E+00
NTH = 2.19E+00	K = 5.00E-03	NO = 1.00E+00	OMEGA = 0.00E+00
OMEGO = 0.00E+00	R1 = 3.20E-01	R2 = 3.20E-01	TAU = 4.19E+00
TAUD = 8.66E-03	TAUP = 4.00E 03	TAUS = 2.00E+00	

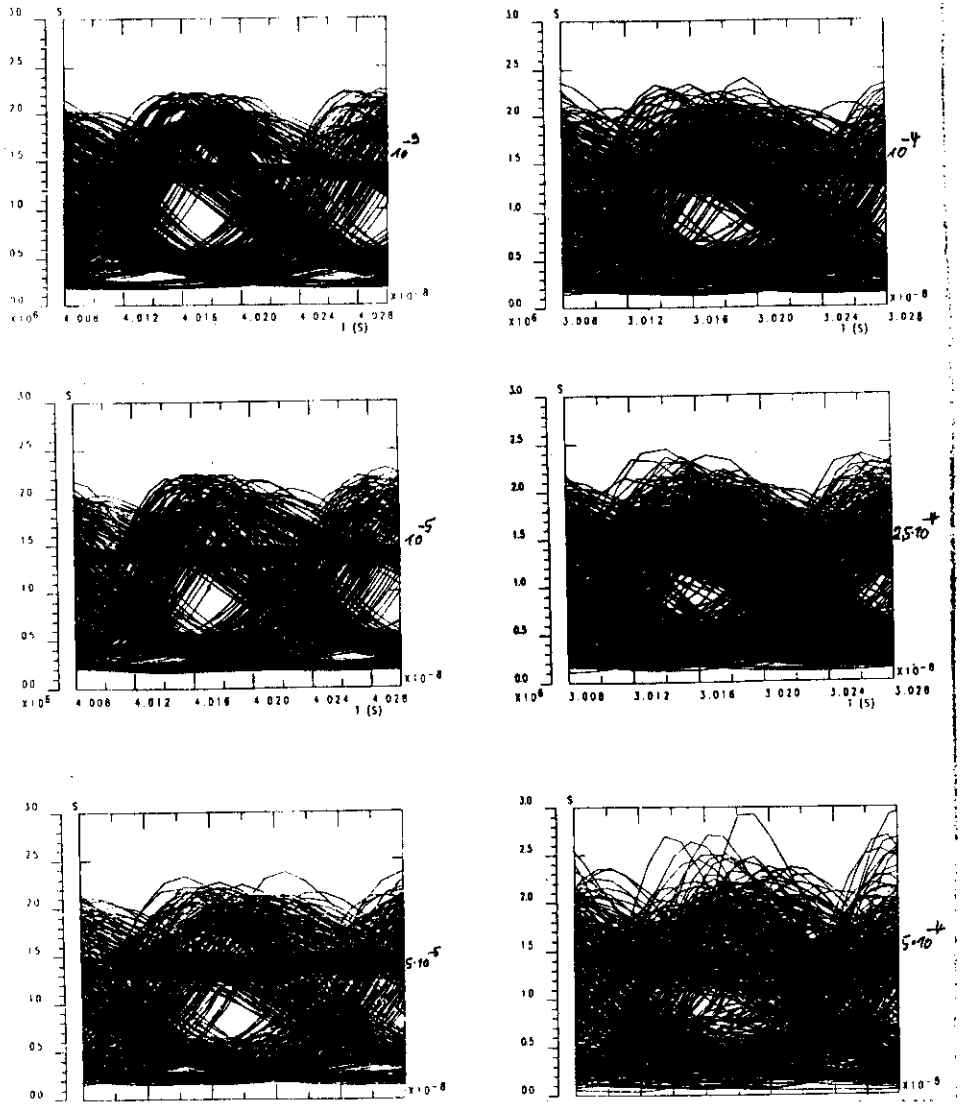

FEEDBACK

Nr 14 8GHz / 55mA / DFB-Typ2

(14)

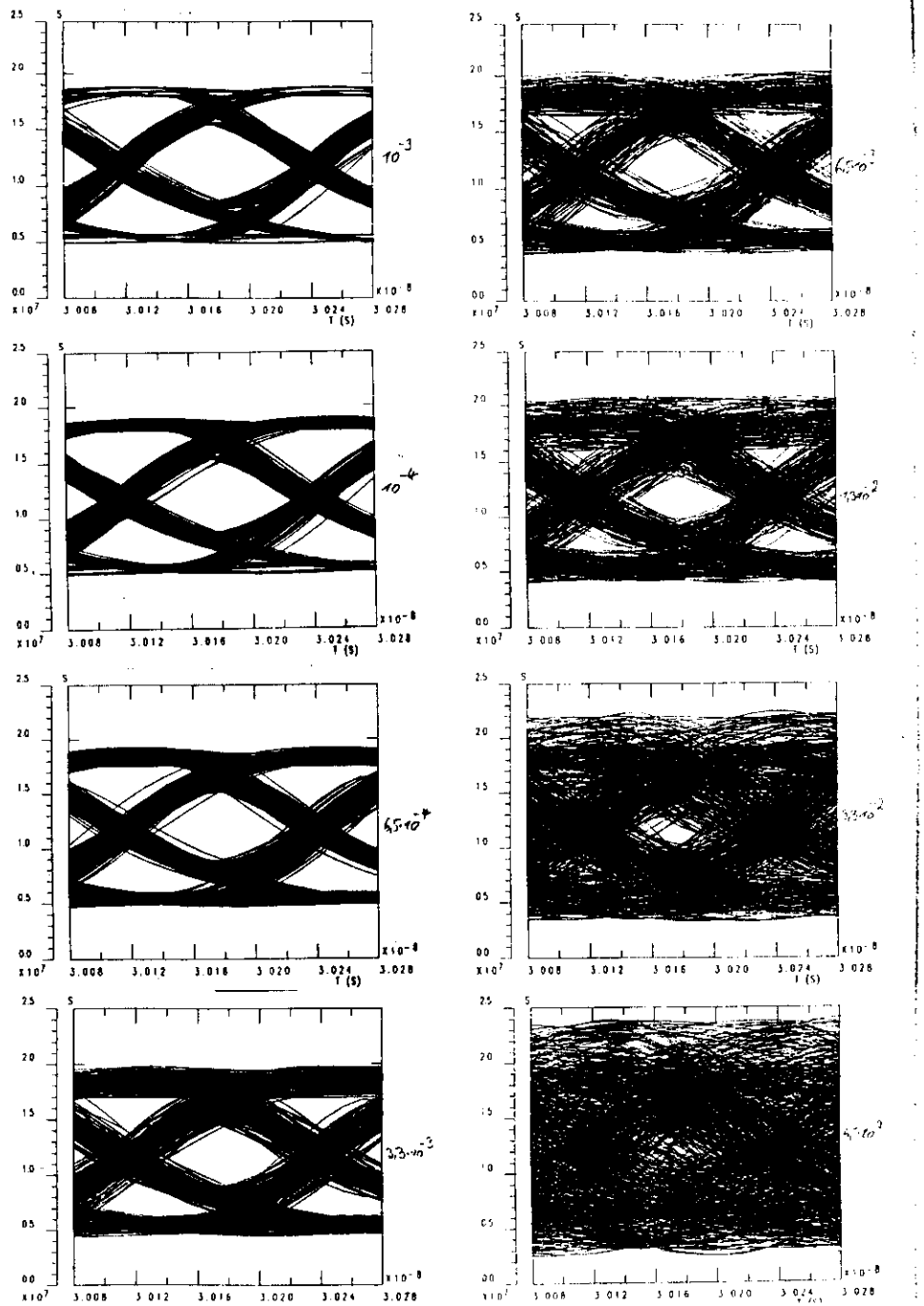

Injection-Locking

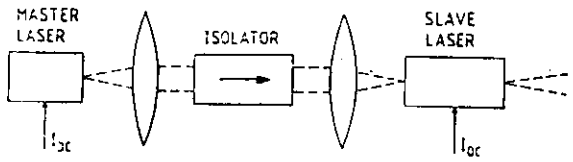

$$\frac{dS}{dt} = (g(n) - \frac{1}{\tau_p})\cdot S + R + F_s +$$

$$+ 2\cdot k_c\cdot\sqrt{S_{inj}\cdot S}\cdot\cos(\Phi_{inj} - \Phi)$$

$$\frac{d\Phi}{dt} = \frac{1}{2}\alpha\cdot\frac{dg}{dn}(n - n_{th}) + F_\Phi -$$

$$- (w_{inj} - w_n(n_{th})) + k_c\cdot\sqrt{\frac{S_{inj}}{S}}\cdot\sin(\Phi_{inj} - \Phi)$$

w_{inj} : MASTER LASER
Φ_{inj} : PHASE OF MASTER
R_2 : INT. REFL. AT INJ. SIDE

k_c : COUPLING CONSTANT $k_c = \frac{1}{\tau_p}\cdot\frac{1-R_2}{\sqrt{R_2}}$

$$\frac{dn}{dt} = \frac{I}{e} - \frac{n}{\tau_s} - g(n)\cdot S + F_n$$

STATIC STABILITY:

$$d < \pm\frac{1}{2\pi}\cdot k_c\cdot\sqrt{S_{inj}/S}\cdot\sqrt{1+[\alpha(1+K\cdot S)]^2} - \frac{1}{2}\alpha\cdot\frac{(1+K\cdot S)}{S}\cdot R$$

ABSOLUTE DYNAMICAL STABILITY:

$$S_{inj}/S < \left[\frac{1}{\tau_p\cdot k_c\cdot\sqrt{1+\alpha^2}}\right]^2$$

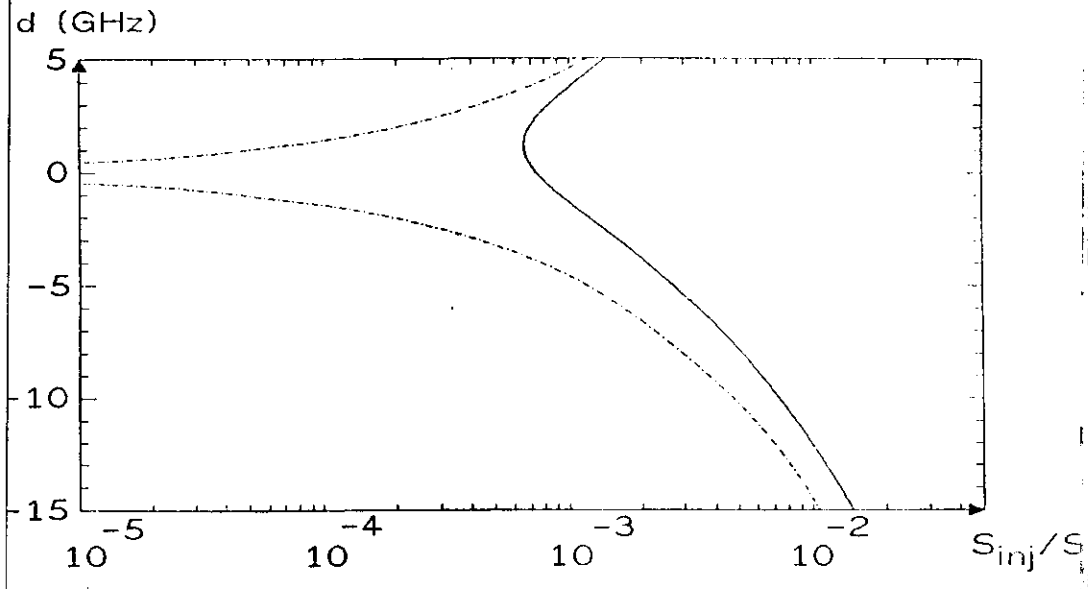

$\alpha = 6$
$A_N = 6600\ s^{-1}$
$I_o = 55$ mA
$n_0 = 1\cdot10^8$
$R_1 = R_2 = 0{,}32$
$K = 5\cdot10^{-8}$
nach einer Simulation
$n_{th} = 1{,}39945\cdot10^8$
$S = 10{,}96\cdot10^5$
$f_r = 6{,}8$ GHz
$f_d = 23{,}4$ GHz
$f_r/f_d = 0{,}29$

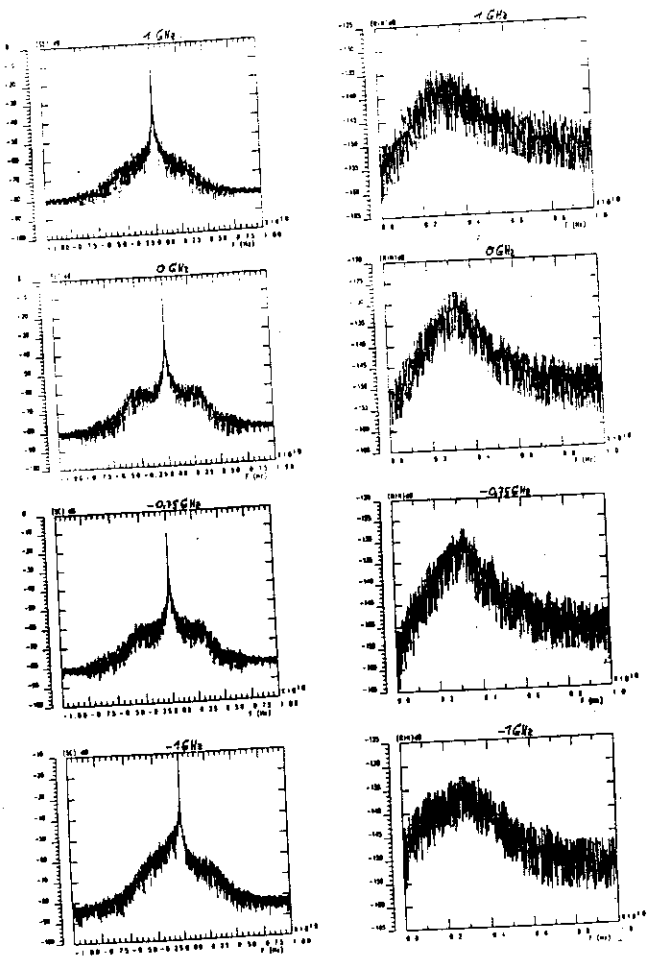
1 GHz
0 GHz
-0.75GHz
-1GHz

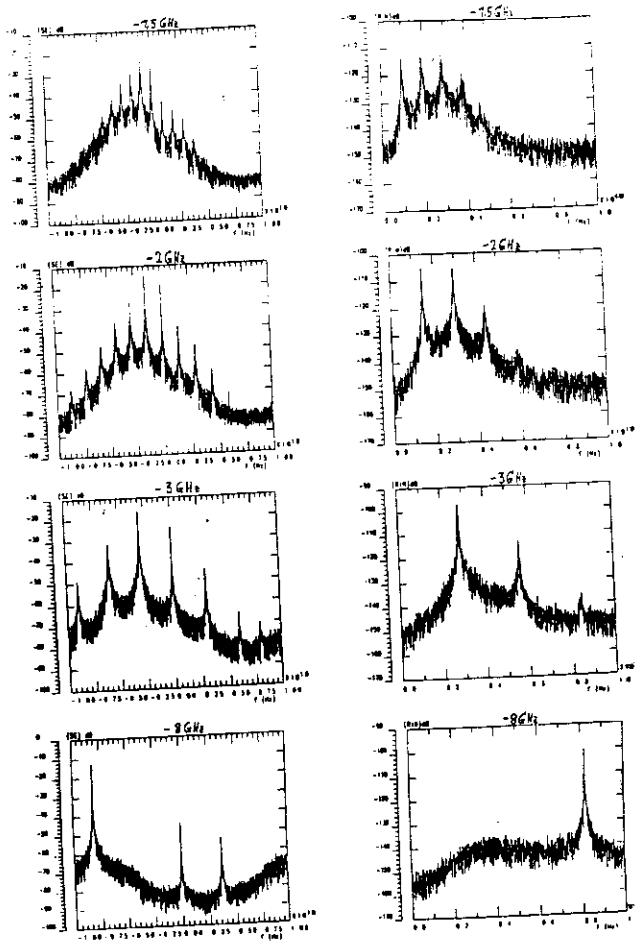
-2.5GHz
-2GHz
-3GHz
-9GHz

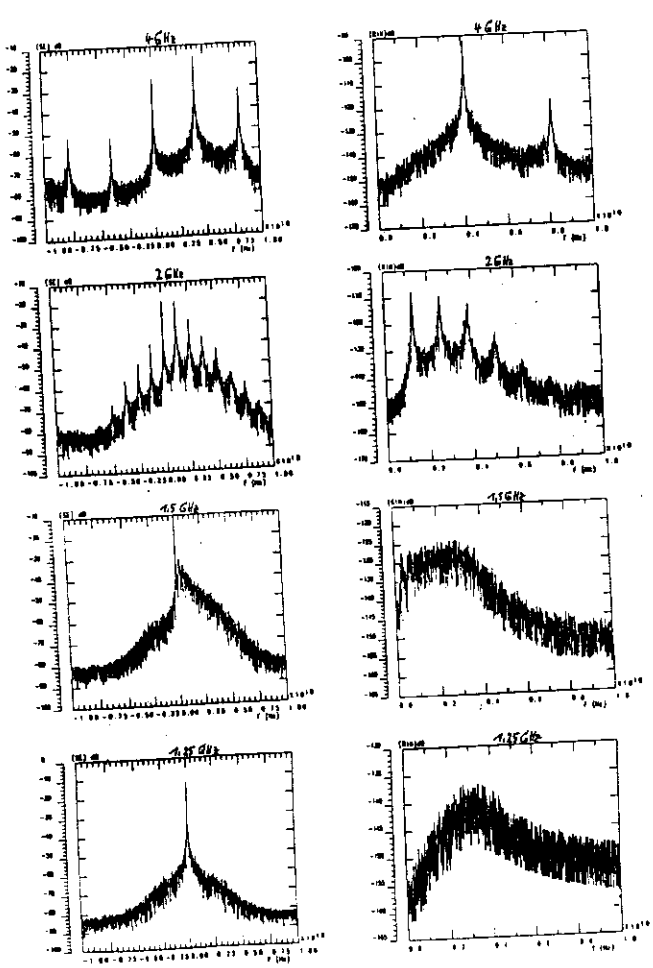
4GHz
2GHz
1.5GHz
1.25GHz

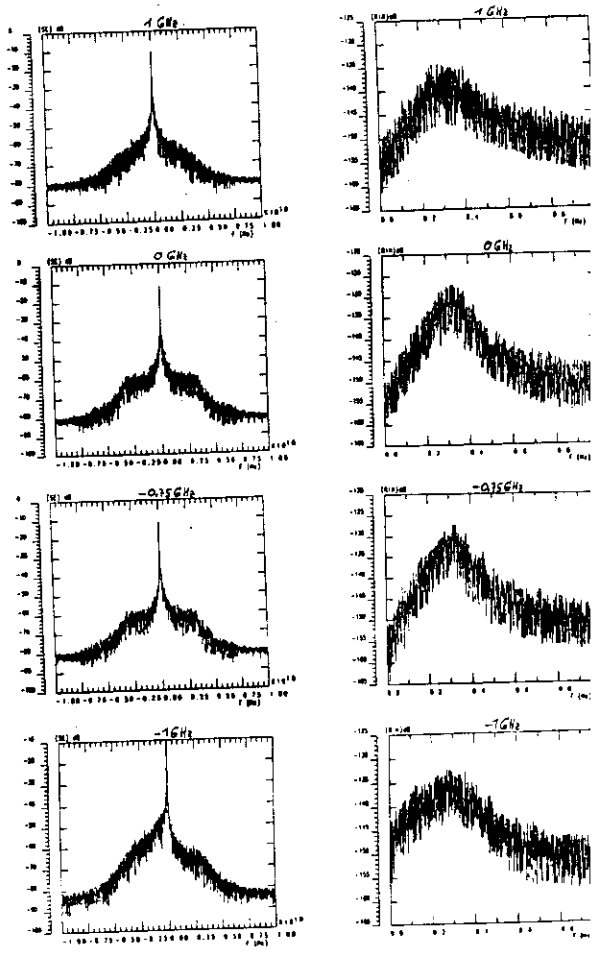
1 GHz
0 GHz
-0.75GHz
-1GHz

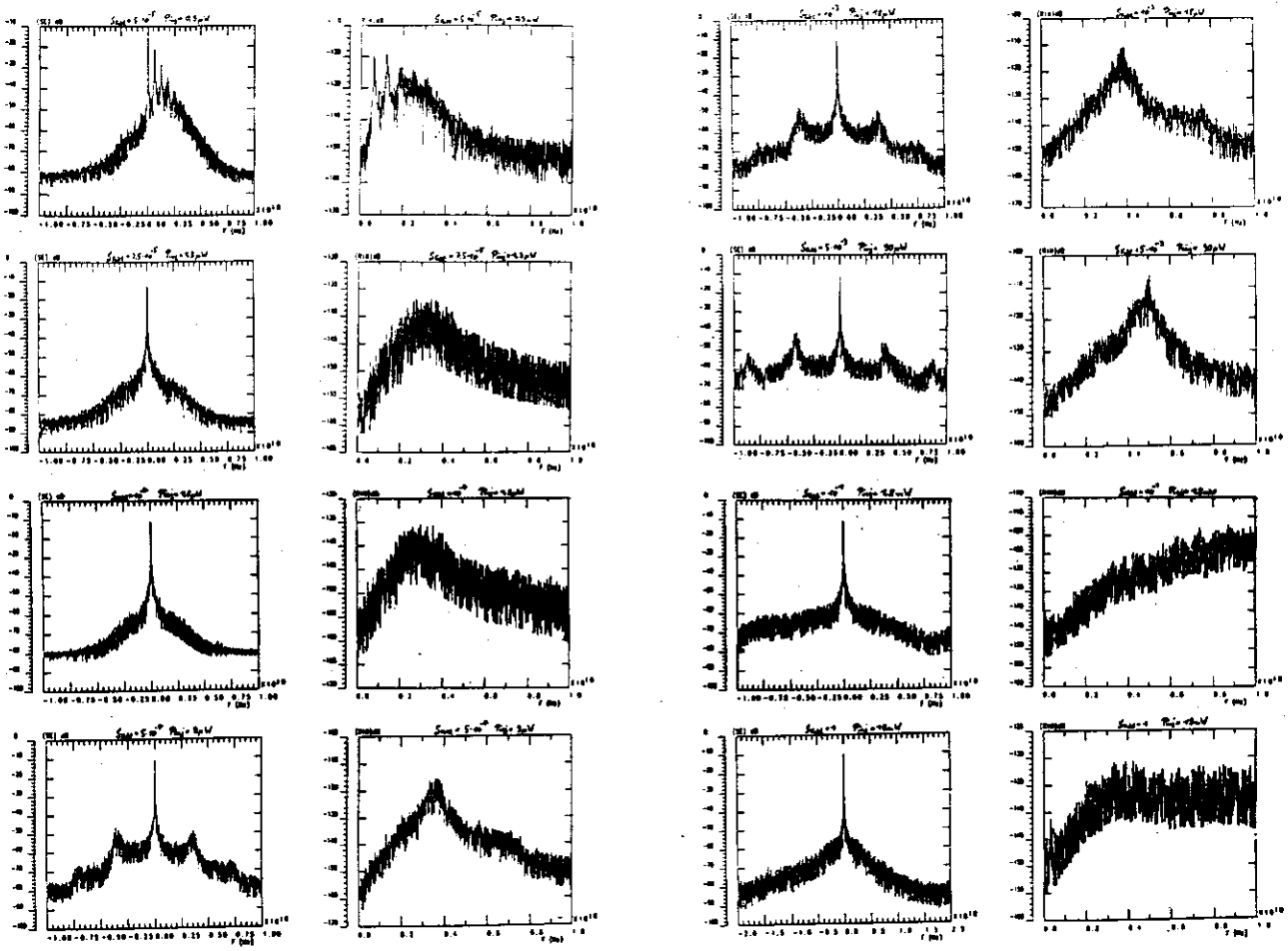

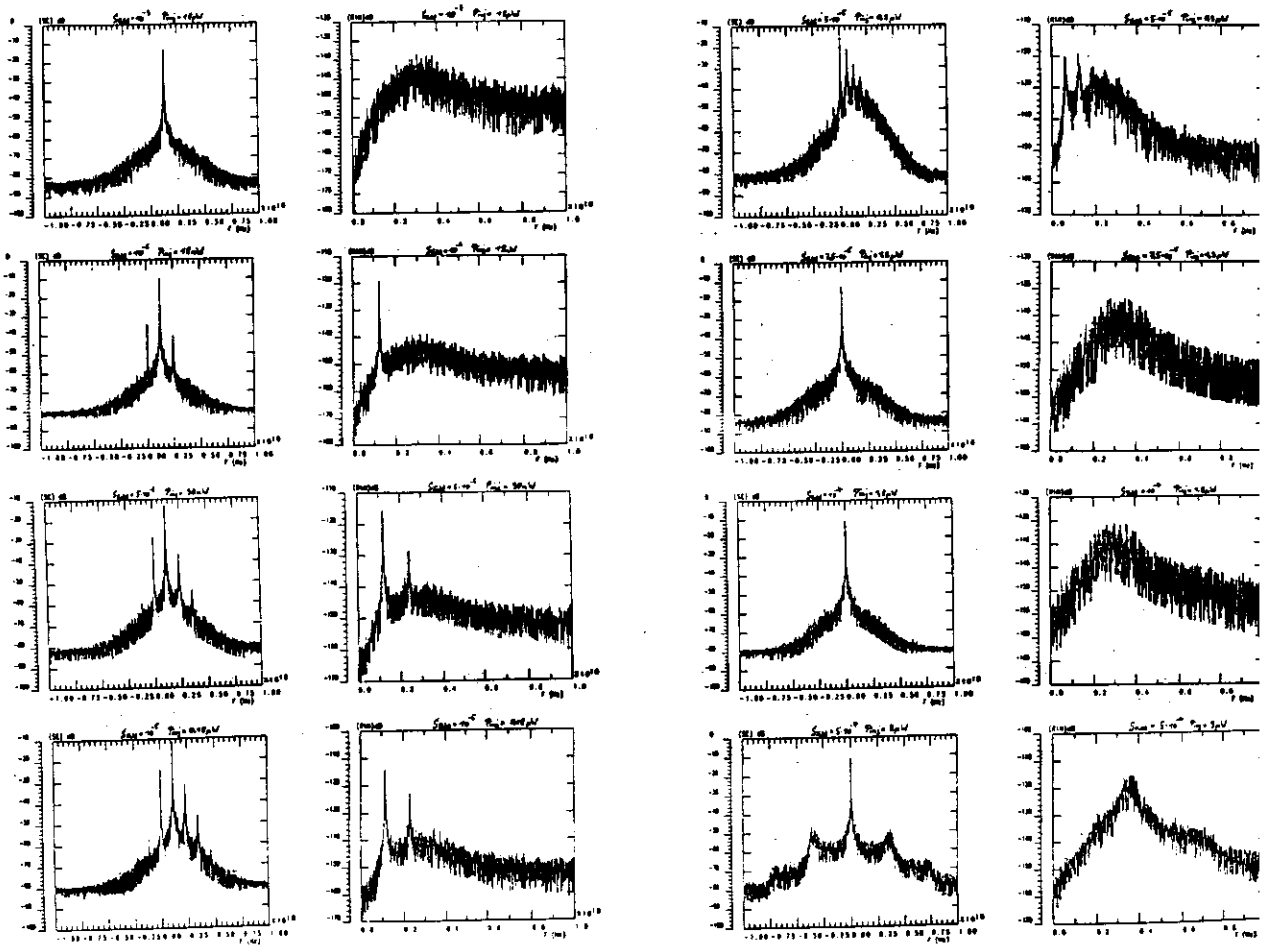

INJ. LOCKING 5Gb/s

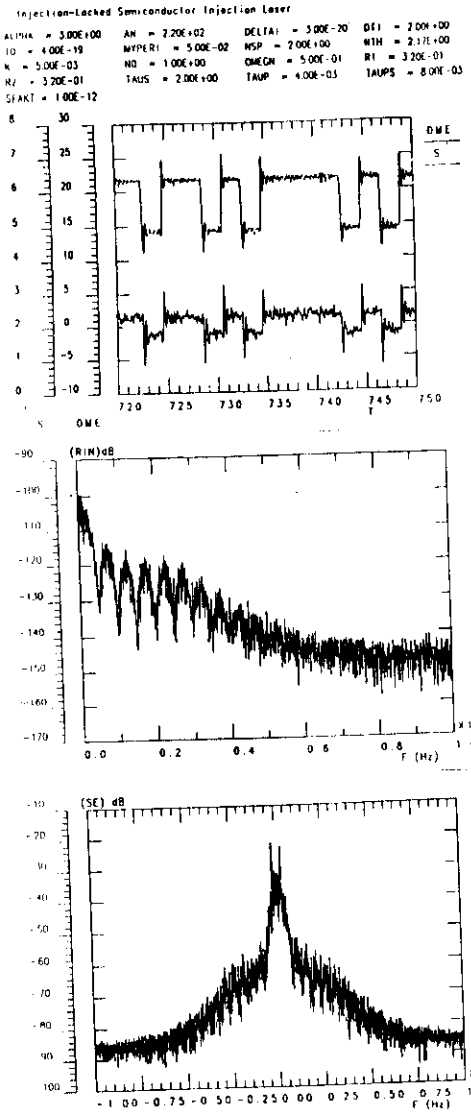

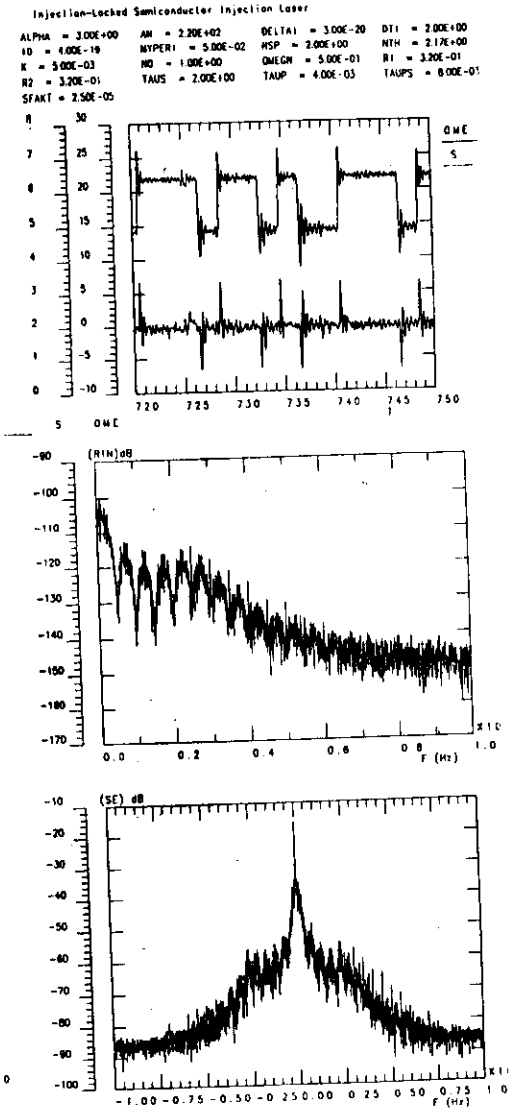

INJ. LOCKED 8 Gbit/s

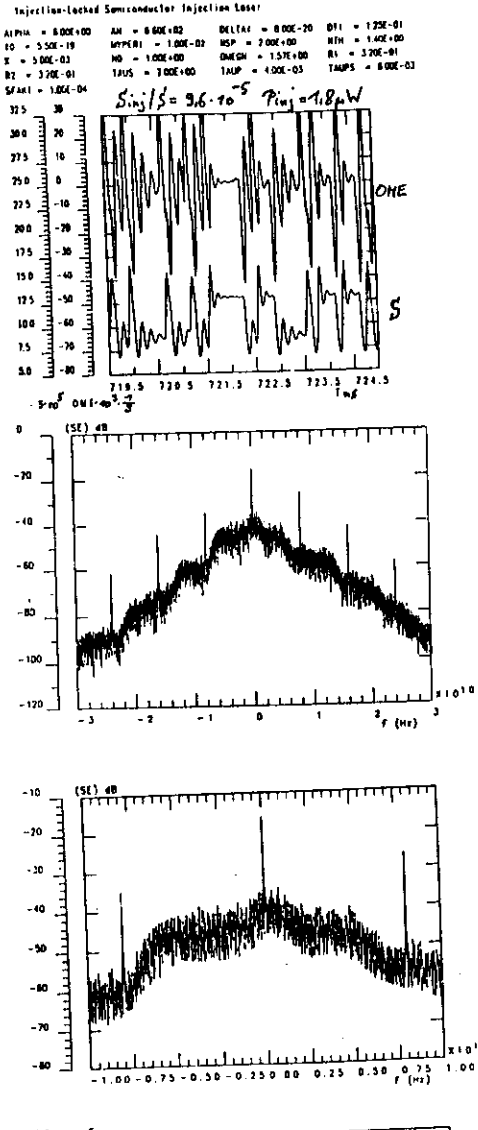

UNLOCKED